

Food web reconstruction through isotopic compositions of fossil faeces: Insights into the ecology of a late Barremian freshwater ecosystem (Las Hoyas, Cuenca, Spain)

Sandra Barrios-de Pedro ^{a, *}, Karyne M. Rogers ^b, Paloma Alcorlo ^c, Ángela D. Buscalioni ^a

^a Unidad de Paleontología and Centro para La Integración en Paleobiología (CIPb), Departamento de Biología, Edificio de Biología, Universidad Autónoma de Madrid, Calle Darwin 2, Cantoblanco, Madrid, 28049, Spain

^b National Isotope Centre, GNS Science, PO BOX 30-312, Lower Hutt, New Zealand

^c Inland-Water Ecosystems Team (I-WET) and Laboratorio de Socioecosistemas, Departamento de Ecología, Edificio de Biología, Universidad Autónoma de Madrid, Calle Darwin 2, Cantoblanco, Madrid, 28049, Spain

ARTICLE INFO

Article history:

Received 18 October 2019

Received in revised form

20 November 2019

Accepted in revised form 28 November 2019

Available online 6 December 2019

Keywords:

Coprolite

Cretaceous

Feeding ecology

Lacustrine

Stable isotopes

ABSTRACT

A total of 54 coprolites with different morphologies from the *Konservat-Lagerstätte* of Las Hoyas (upper Barremian, Cuenca, Spain) were analysed for stable isotopes ($\delta^{15}\text{N}$ and $\delta^{13}\text{C}_{\text{org}}$) to examine the food-web structure of this ancient wetland. The Las Hoyas wetland exhibited wetter and drier periods that indicated water table oscillations. Differences in the $\delta^{15}\text{N}$ values of coprolites collected from wetter and drier facies were probably due to different baseline $\delta^{15}\text{N}$ values during the dry periods (higher) compared to those of the wetter periods. The $\delta^{13}\text{C}_{\text{org}}$ values indicated that aquatic food resources were the most commonly used by the animals from Las Hoyas. Assuming a Trophic Enrichment Factor (TEF) of + 2.5 ‰, three trophic levels were established for the coprolite association. All the specimens of circular, ellipsoidal, elongated, and rosary morphotypes fell into the same trophic level, whereas other morphotypes (cylinder, irregular, and thin lace) exhibited a wide range of $\delta^{15}\text{N}$ values and the highest % N concentrations. The covariation between $\delta^{15}\text{N}$ and $\delta^{13}\text{C}_{\text{org}}$ values describe a wide spectrum of values across the middle and upper part of the ecosystem's food web structure, suggesting that the Las Hoyas ecosystem hosted specialist feeders and omnivorous and/or opportunistic feeders, the latter being the majority. The variation of $\delta^{15}\text{N}$ values within the specimens of some morphotypes showed that the larger coprolites do not exhibit any correspondence between the faecal size and $\delta^{15}\text{N}$ values.

© 2019 Elsevier Ltd. All rights reserved.

1. Introduction

The late Barremian fossil site of Las Hoyas (La Huérguina Formation, Cuenca, Spain) is a well-known exceptional deposit that has yielded abundant body and trace fossils. The biota is represented by a wide diversity (currently estimated at about 200 species; Buscalioni and Poyato-Ariza, 2016) of Eubacteria, Chlorobionta (including high diversity of Charophyta and Embryophyta), Protostomia (including a high diversity of Arthropoda), and Vertebrata. Insects and fishes showed the greatest percentage of families, whilst ostracods and molluscs were the next greatest in terms of

diversity (Buscalioni et al., 2016). The Las Hoyas *Lagerstätte* was deposited around 126 Ma, and the locality represented a single pond within a regional system of wetlands. Almost 2000 specimens comprise the coprolite collection from this locality, and twelve different morphotypes have been described, mostly produced by ichthyophagous animals (Barrios-de Pedro et al., 2018). Coprolites are particularly useful to infer digestive strategies, the diet of animals, predator-prey interactions, faunal abundance and the possible food webs of ancient ecosystems (e.g. Chin and Gill, 1996; Chin et al., 1998; Rodríguez-de la Rosa et al., 1998; Northwood, 2005; Peñalver and Gaudant, 2010; Barrios-de Pedro and Buscalioni, 2018). The Las Hoyas coprolites are rich in undigested remains, and based on the taphonomic properties of the inclusions, Barrios-de Pedro and Buscalioni (2018) provided information about digestive strategy patterns of the Las Hoyas animals. The present contribution renders an analytical description of the Las

* Corresponding author.

E-mail addresses: sbarriosdepedro@gmail.com (S. Barrios-de Pedro), K.Rogers@gns.cri.nz (K.M. Rogers), paloma.alcorlo@uam.es (P. Alcorlo), angela.delgado@uam.es (Á.D. Buscalioni).

Hoyas coprolites by considering the stable carbon and nitrogen isotope values ($\delta^{13}\text{C}$ and $\delta^{15}\text{N}$) of the different morphotypes in order to provide a new dietary information about the trophic web of this Barremian freshwater ecosystem.

Only a few stable isotope studies using $\delta^{13}\text{C}$ and $\delta^{15}\text{N}$, have been undertaken for Mesozoic fossils, in part due to the perception that diagenesis has obscured all potential primary signal (Fricke et al., 2008). The scarce number of contributions is even more notorious in the case of coprolites, represented by the analyses of a single to several specimens. Isotopic values have been reported in coprolites attributed to titanosaurs from the Late Cretaceous Lameta Formation in India (Ghosh et al., 2003). In these coprolites, the carbon and nitrogen isotopic ratios were compared to the content in bone collagen of extant carnivorous and herbivorous animals and faeces. Another study (Bajdek et al., 2014) determined carbon and nitrogen isotopes of three Late Triassic dicynodont coprolites from Poland, and compared their findings with other published results (see fig. 12 in Bajdek et al., 2014). Stable isotopes have been successfully used to describe ancient food webs from an exceptional Eocene deposit at Messel, and the Oligocene Enspel site (Schweizer et al., 2006, 2007). Following these approaches, which provided sufficient evidence that isotope ratios of solid excreta was directly correlated to animal tissues (Vander Zanden and Rasmussen, 2001), we explored the coprolite association of Las Hoyas aiming to discover the dietary niches of the coprolite producers. The $\delta^{15}\text{N}$ and $\delta^{13}\text{C}$ values of each coprolite morphotype were used to obtain an estimate of the food-web structure and available food resources in the Las Hoyas wetland.

Stable isotopes provide a quantitative measure of the food chain length, the identification of the trophic level of an organism, and the origin of the primary productivity of the system (Vander Zanden et al., 1999; Eggers and Jones, 2000; Post, 2002; Wolf et al., 2009). The trophic level of an organism can be inferred by studying its $\delta^{15}\text{N}$ isotopic signal, owing to the preferential excretion of light ^{14}N as a by-product of protein synthesis, leaving the animal enriched in ^{15}N relative to its diet (Kling et al., 1992). The difference in the nitrogen isotope ratio of a consumer and its diet is known as the 'trophic enrichment factor' (TEF) and has a fractionation from +1 to +5‰. It assumes an average of +3.4‰, after accounting for many taxa (DeNiro and Epstein, 1981; Minagawa and Wada, 1984; Kling et al., 1992; Vander Zanden and Rasmussen, 2001; Post, 2002; Vanderklift and Ponsard, 2003; Vander Zanden and Fetzer, 2007). In turn, the $\delta^{13}\text{C}$ values give information about the dietary sources of the animal. Carbon isotope ratios fractionate very little in the food web with minimal change for each trophic step (~ 0 – 1 ‰) (DeNiro and Epstein, 1978; Schoeninger and DeNiro, 1984; Ambrose and DeNiro, 1986; Vander Zanden and Rasmussen, 2001; Post, 2002; Caut et al., 2009). Therefore, it is not a suitable measurement to infer the trophic position of an organism, but it is useful to track the origin of a consumer's nutrients (Post, 2002). It may be inferred whether the animal fed on C3 plant ($\delta^{13}\text{C}_{\text{org}}$ values between -24 and -34 ‰) or C4 plants ($\delta^{13}\text{C}_{\text{org}}$ values between -6 and -19 ‰) (DeNiro and Epstein, 1978), as well as the relative contribution of terrestrial or aquatic sources. Faeces and the whole-body carbon usually have slightly more positive $\delta^{13}\text{C}$ values than the ingested food sources (DeNiro and Epstein, 1978).

Stable isotope signatures measured in autolithified soft organic material, such as coprolites, have demonstrated that the isotope enrichment in fossils is preserved over geologic time-scales (Schweizer et al., 2006). Instead of isolated individual examples, we explore herein a coprolite association to reconstruct the food-web structure of an ancient ecosystem. The association represents a complex collection of faeces produced by vertebrate organisms in a freshwater wetland with subtle different temporal and spatial

scales. The outcome from this study will enhance our knowledge on Mesozoic ecosystems validating the extent that coprolites preserve their isotopic signatures, in order to understand the complex nature of the Las Hoyas aquatic food web.

2. The Las Hoyas deposit

2.1. Location and geological setting

The Las Hoyas fossil site ($40^{\circ}5'35.85''\text{N}$ $1^{\circ}53'25.19''\text{W}$) is located in the southwestern Iberian Range (Serranía de Cuenca, Spain). It is a Lower Cretaceous fossil site, Barremian in age, which belongs to La Huérguina Limestone Formation of the Southwestern Iberian Basin domain (Fregenal-Martínez et al., 2017) (Fig. 1). The site's age (126.3–129.4 Ma) was determined on the basis of the charophytes and ostracods association (Diéguez et al., 1995; Vicente and Martín-Closas, 2013; Fregenal-Martínez et al., 2017). A second rifting cycle during the Late Jurassic–Early Cretaceous related to the opening of the central Atlantic and the rotation of the Iberian Plate induced the development Southwestern domain in the Iberian basin (Fregenal-Martínez and Meléndez, 2016). Extensional tectonics in turn divided each domain into several basins of graben and half-graben type.

The southwestern domain in the Serranía de Cuenca Basin does not record any sedimentation for approximately 30 myr (Oxfordian–lower Barremian), resulting in the development of a prominent regional unconformity (Vicente and Martín-Closas, 2013). The upper Barremian continental deposits were found to include alluvial, lacustrine, and palustrine sedimentary settings. In the Serranía de Cuenca, the thickest record of these non-marine deposits (400 m) was found in the Las Hoyas Basin, and a vertical sequence made up of two lithostratigraphic units that are laterally connected, Tragacete and La Huérguina Formations, has been proposed (Fregenal-Martínez, 1998; Fregenal-Martínez and Meléndez, 2000, 2016; Fregenal-Martínez et al., 2017) (Fig. 1). The La Huérguina Formation, where the locality of Las Hoyas is placed, is mainly developed at the top of the sequence and it is primarily composed of a wide variety of limestone facies, with minor amounts of marl, sandy limestone and local lignite.

2.2. Palaeoenvironmental context

The palaeogeographical setting of the southwestern Iberian domain at the Serranía de Cuenca was constrained by tectonics, climate, and the composition and distribution of the substrate in the source areas. Sea level did not influence sedimentation, since the Serranía de Cuenca did not receive any direct marine influence (Fregenal-Martínez, 1998; Poyato-Ariza et al., 1998; Bailleul et al., 2011; Fregenal-Martínez et al., 2014; Fregenal-Martínez and Meléndez, 2016). Climate was the most relevant palaeogeographical constraint. The Barremian–Aptian regional climate has always been considered seasonal subtropical with alternating wet and dry seasons. The palaeogeography and palaeoclimate of Iberia in the Western Tethys set the plate at the dry, divergent subtropical zone assuming a seasonal warm and semi-arid subtropical climate for the Early Cretaceous (Ziegler et al., 1987).

The La Huérguina Limestones Formation records sedimentation in poorly drained areas, where lacustrine conditions prevailed with a minor influx of allochthonous sediments (Fregenal-Martínez and Meléndez, 2016). Its depositional system has been interpreted as an inland freshwater system of wetlands at a regional scale (Fregenal-Martínez et al., 2017). The complete isolation from marine influence is also supported by geochemical data carried out in the laminated limestones (Talbot et al., 1995; Poyato-Ariza et al., 1998; Fregenal-Martínez et al., 2014). Low strontium isotopic ratios (mean $^{87}\text{Sr}/^{86}\text{Sr}$

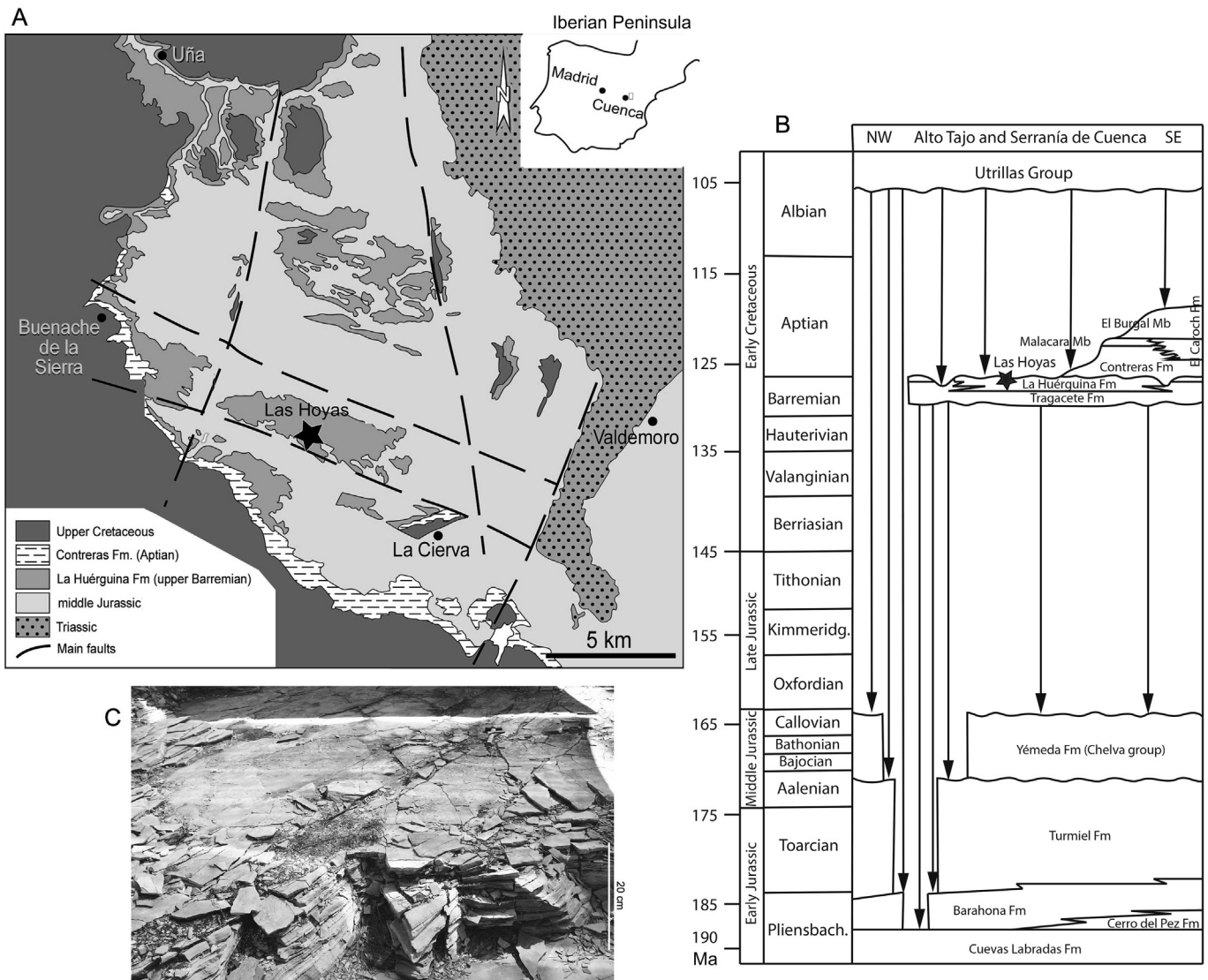


Fig. 1. Geological context of the Las Hoyas fossil site. (A) General geological map of the central area of the Southwestern Iberian Range at Serranía de Cuenca (east of the city of Cuenca) indicating the upper Barremian locality of Las Hoyas with a star (modified from [Fregenal-Martínez and Meléndez, 2000](#)). (B) Lithostratigraphic scheme proposed by [Fregenal-Martínez et al. \(2017\)](#). The locality of Las Hoyas is marked with a star. (C) View of the Las Hoyas laminated limestones (La Huérguina Formation).

value ~ 0.07) determined in the La Huérguina Jurassic and Barremian carbonates, and in large bones of pycnodontiforms and coelacanths fishes, indicated that these fishes grew and inhabited freshwater without marine influence (see fig. 5 in [Poyato-Ariza et al., 1998](#)).

The Las Hoyas fossiliferous site is characterized by deposits of finely laminated limestones, which are composed almost entirely of calcium carbonate, with a small fraction of clays and organic matter ([Fregenal-Martínez and Meléndez, 2016](#)). The $\delta^{13}\text{C}$ and $\delta^{18}\text{O}$ values ($\delta^{13}\text{C} = -2.72 \pm 0.23\text{‰}$; $\delta^{18}\text{O} = -4.81 \pm 0.17\text{‰}$) and their covariances, collected from a 1.25 m thick section of laminated limestones at the fossil site, indicated the prevalence of lacustrine conditions in a groundwater-dominated, relatively small, hydrologically open lake ([Poyato-Ariza et al., 1998](#)). The same results were obtained by analysing rare elements in fossils of terrestrial organisms, such as dinosaurs, turtles and lizards (La/Yb, with values from 0.61 to 0.34, and La/Sm with values from 0.20 to 0.44), explained as the post-mortem incorporation of carcasses within the freshwater-river domain of the Las Hoyas wetland ([Bailleul et al., 2011](#)).

2.3. The Las Hoyas fossil site

The fossil site has been the subject of layer-by-layer excavations since 1991. Small squares with an average surface area of about 30 m^2 are deemed suitable for testing the homogeneity of the fossil association throughout the layers. The excavation method controls the palaeontological and sedimentological information, in such a way that the fossil content of the layers can be related to the features of the corresponding microfacies. The laminated limestones of Las Hoyas reflect two differentiated petrographic microfacies associations ([Fregenal-Martínez, 1998](#)). One group of microfacies was the result of sedimentation by traction and decantation of the allochthonous elements (e.g. detrital carbonate particles, plant debris) and bio-induced calcium carbonates that were deposited during seasonal flooding and longer-term wetter periods. The other group was autochthonously-produced microfacies composed of carbonates generated by the growth of thick mats of microbial communities during drier periods ([Fregenal-Martínez, 1998](#)). During these drier periods, the depth of the water column was reduced to probably just a few centimetres. These two contrasting periods

incorporated differences in the abundance, content, and preservation quality of the fossils. The wetter types of microfacies were dominated by insects and large body-size fishes, with fossil associations rich in diversity, but low in fossil abundance. The drier types of microfacies were dominated by ostracods greater in relative abundance than crustaceans (shrimps and crayfish) and juvenile fishes. These exhibited a higher number of fossils, being less diverse in taxa (Buscalioni and Fregenal-Martínez, 2010). By considering the sedimentation and preservation of laminated sediments and fossils, it was interpreted that the fossiliferous laminations were produced in a shallow marginal lacustrine environment with seasonal water-level oscillations, which was filled with layered microbial mats (Fregenal-Martínez and Meléndez, 2016). Microbial mats, found both in laminated limestones and fossils, were considered the key to understanding fossil preservation in Las Hoyas (Briggs et al., 1997, 2016; Iniesto et al., 2013, 2016, 2018).

The Las Hoyas fossil record has a high spatial fidelity, and it consists mostly of demic and autochthonous fossils, mostly dominated by aquatic organisms (>80 %). It also has a high temporal fidelity with assemblages found in continuity. Therefore, the fossil associations were not linked to any particular catastrophic event(s), but to the alternating seasonal periods of the original palaeoecosystem (Buscalioni and Fregenal-Martínez, 2010; Buscalioni and Poyato-Ariza, 2016).

3. Material and methods

3.1. Coprolites

The Las Hoyas (LH) fossil collection is housed at the Museo de Paleontología de Castilla-La Mancha (MUPA) in Cuenca (Spain). The fifty-four coprolites analysed were recovered from a measurable surface of several hundred square meters, and from a sedimentary record of less than 10 m thick. Thirty-one coprolites came from taphonomically controlled layers, with five coprolites coming from wetter microfacies, and twenty-six coprolites from drier layers. The remaining twenty-three coprolites lacked this sedimentological information. Coprolites from the wetter microfacies were compared to drier ones in order to test if there was any significant isotopic difference.

The fifty-four coprolite specimens analysed were selected based on the morphological classification proposed by Barrios-de Pedro et al. (2018) (Appendix A). The sample set comprised 10 cylinder, 1 circular, 4 cone, 2 ellipsoidal, 2 elongated, 10 irregular, 9 thin lace, 2 bump-headed lace, 4 straight lace, and 1 rosary-like morphotypes (Fig. 2). Moreover, 9 broken coprolites were also processed. The irregular morphotype is classified as a compilation of specimens that cannot be assigned any morphology because they encompass different shapes and external features. The most frequent length of the Las Hoyas coprolites is between 10 and 40 mm, so those coprolites with both lengths > 40 and widths > 10 mm are herein treated as large coprolites (Fig. 3).

The coprolite morphotypes were grouped into three clusters based on their relative proportions according their lengths and widths (Figs. 2 and 3) and shapes. The first group (G1) gathers relatively long coprolites, 17 times longer than their width on average, and this group contains the bump-headed lace, rosary, straight lace, and thin lace morphotypes. This set is linked to coprolite producers with not-so effective digestive processing, and shows a greater than average amount of undigested fragments of organic matter (i.e. bones, scales, thin laminae of crustaceans) (Barrios-de Pedro and Buscalioni, 2018). The second group (G2) is formed by coprolites 3 times longer than their width on average,

and comprises circular, cone, cylinder, ellipsoidal, and elongated morphotypes. The group is linked to coprolite producers with longer digestive processes, showing fewer undigested fragments that in turn are more altered. The third group (G3) includes irregular and broken coprolites which are 3 times longer in average (Appendix B). The group contains a diversity of cases but generally comprises coprolites with visible inclusions, which, in turn, are very damaged by digestive process, and some specimens have no visible inclusions at a macroscale (Barrios de Pedro and Buscalioni, 2018). We interpreted differences in the number of inclusions for G1, G2, and G3 as the outcome of distinct digestive processes, also including different feeding habits and the possible food resistance to digestive acids (Bajdek et al., 2017).

3.2. Diagenetic alteration and taphonomy of the coprolites

The Las Hoyas coprolites are exceptionally well-preserved, maintaining their shapes, original contour, and volume (Fig. 2). The taphonomic features of these coprolites show that their integrity, absence of desiccation marks, and volume are congruent with faeces produced and deposited in an aquatic environment that soaked before burial in carbonate alkaline water (Barrios-de Pedro et al., 2018). The mineralogical composition of the coprolites analysed by X-Ray Powder Diffraction (XRD) contains apatite group compounds $\text{Ca}_5(\text{PO}_4)_3$ (hydroxylapatite sulfonated and carbonate orthophosphates with incorporation of elements such as fluoride) and calcium carbonate CaCO_3 (Table 1). The acquisition of fluoride can occur by ion exchange with groundwater and it does not require recrystallization or deposition of new mineral phases (Hollocher et al., 2010; Hollocher and Hollocher, 2012). Energy Dispersive X-ray (EDX) analyses show that major elemental differences are primarily found for P contents in coprolites, and in Ca, C, Al, and Si contents in limestones (Table 2). A subtle alteration on the original chemical composition is probable because hydroxylapatite sulfonated is an intermediate phase of degraded apatite (Sugama and Pyatina, 2018). However, there was no secondary precipitation or recrystallization in the coprolites, and the coprolite matrix is a uniform microcrystalline phosphatic matrix (Barrios-de Pedro, 2019), as occurred in other Cretaceous coprolites from Montana, which points to the exceptional preservation of the fossils (Hollocher et al., 2010). Therefore, it is expected that diagenesis has not entirely obscured the original stable isotope values (See Appendix C for a detailed explanation).

3.3. Stable isotopic analyses of the coprolites

The coprolites were carefully extracted from the host rock using a punch, and they were finely ground and homogenised using a mortar and pestle. All tools used during the extraction and preparation of the coprolites were carefully cleaned with ethanol 70 %, and then rinsed three consecutive times using deionized water Milli-Q between samples to avoid cross-contamination. Once extracted, around 10 mg of powdered coprolite was weighed into 6×4 mm tin capsules, and then analysed in duplicate (when enough material was available) using an elemental analyser—*isotope ratio mass spectrometer* (EA-IRMS).

Stable carbon and nitrogen isotopes, and the total carbon and nitrogen elemental composition were measured for every coprolite at the Stable Isotope Laboratory, GNS Science in Lower Hutt, New Zealand, using an Eurovector elemental analyser (in continuous-flow mode) coupled to an Isoprime isotope ratio mass spectrometer.

Carbon and nitrogen isotopes, % C and % N, were determined firstly on the untreated bulk samples (precision of ± 0.2 ‰ for $\delta^{13}\text{C}$,

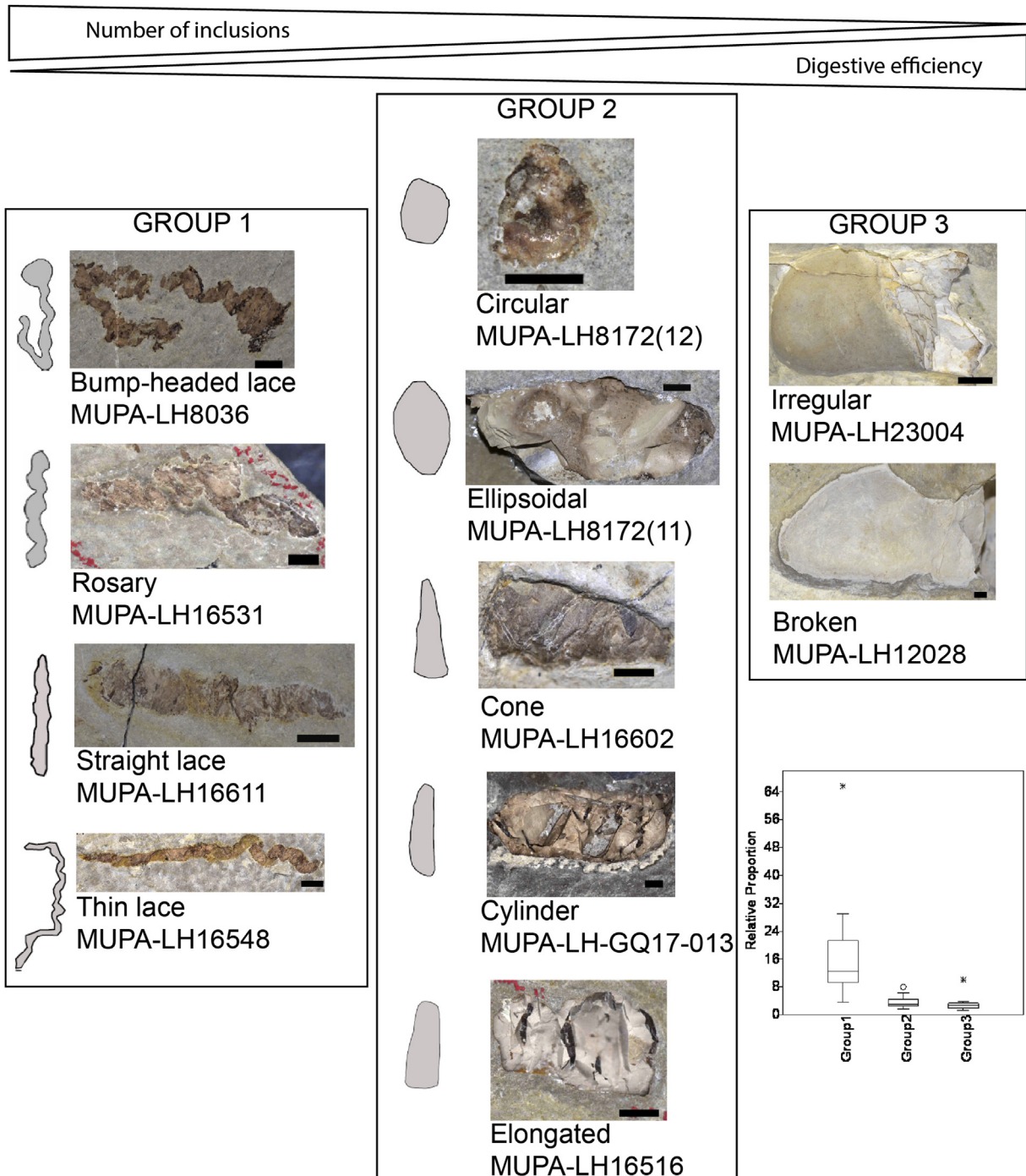


Fig. 2. Groups of coprolite morphotypes from Las Hoyas. The three groups of morphotypes with macroscopic photos and outlines of a representative specimen of each morphotype. On the top, a trend relating number of inclusions and digestive efficiency; on the bottom, a box-plot representing the relative proportions (relative diameter) per morphotype group. The main boxes represent the quartiles; and the line inside is the median; the whiskers represent minima and maxima values; the crosses and circles represent outliers. Scale bars of each photos = 2 mm, except for the irregular coprolite MUPA-LH23004 (scale bar = 10 mm).

± 0.1 % for C, ± 0.3 ‰ for $\delta^{15}\text{N}$, and ± 0.02 for % N), to minimise any unintended nitrogen fractionation that can occur with HCl treated samples and potentially affect the trophic position estimation (Kolasinski et al., 2008; Schlacher and Connolly, 2014). The results were expressed in delta notation (δ), defined as ‰, according to the equation

$$\delta X = [(R_{\text{sample}}/R_{\text{standard}}) - 1] \quad (1)$$

by Coplen (2011), where 'R' is the ratio of heavy to light isotope ($^{13}\text{C}/^{12}\text{C}$ and $^{15}\text{N}/^{14}\text{N}$) in the sample (R_{sample}) and the standard (R_{standard}). The $\delta^{13}\text{C}_{\text{tot}}$ and $\delta^{15}\text{N}$ ratios were determined and normalised to internal working reference materials with the following measured values: leucine, -28.30 ‰ for $\delta^{13}\text{C}$, $+6.54$ ‰ for $\delta^{15}\text{N}$; cane sugar, -10.33 ‰ for $\delta^{13}\text{C}$; caffeine, -38.17 ‰ for $\delta^{13}\text{C}$, -7.82 ‰ for $\delta^{15}\text{N}$; beet sugar, -24.58 ‰ for $\delta^{13}\text{C}$; EDTA, -31.12 ‰ $\delta^{13}\text{C}$, $+0.58$ ‰ for $\delta^{15}\text{N}$; Acetanilide, -30.8 ‰ for $\delta^{13}\text{C}$, -2.3 ‰ for $\delta^{15}\text{N}$; and IVA

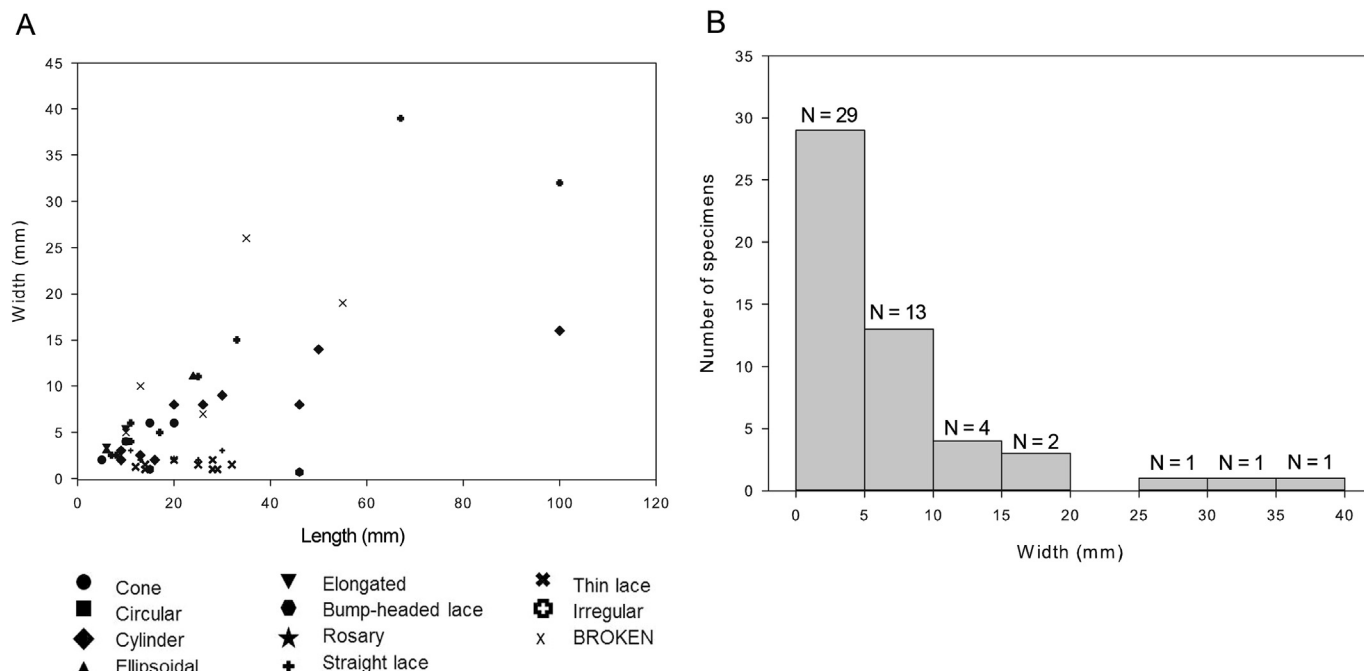


Fig. 3. Size of the coprolites analysed. (A) Scatterplot between the width and length of each coprolite morphotype. (B) Histogram showing the number of coprolites per 5 mm of width interval.

Table 1
X-Ray Powder Diffraction (XRD) analyses performed on coprolites and limestones from Las Hoyas. The 'X' indicates the presence of the mineralogical compound in the coprolite matrix or in the limestone. Abbreviations: BS: Barium Sulfate, Ba(SO₄); C: Carbon, C; CC: Calcium Carbonate, CaCO₃; CPFC: Calcium Phosphate Fluoride Carbonate, Ca_{9.74}(PO₄)_{5.45}F_{2.05}(CO₃)_{0.53}; CPSH: Calcium Phosphate Sulfate Hydroxide, Ca_{4.95}(PO₄)_{2.9}(SO₄)_{0.1}(OH); CPSL: Sodium Calcium Magnesium Fluoride Carbonate Phosphate Sulfate, Na_{0.19}Ca_{4.78}Mg_{0.04}(PO₄)_{2.41}(CO₃)_{0.473}(SO₄)_{0.1}F_{1.17}; SO: Silicon Oxide, SiO₂; ZnS: Zinc Sulfide, ZnS.

Specimen Number	Nature	CPFC	CPSH	CPSL	CC	BS	C	SO	ZnS	Facies
MUPA-LH9195	Coprolite			x	x					Unknown
MUPA-LH9651	Coprolite		x		x	x				Unknown
MUPA-LH7202	Coprolite		x							Unknown
MUPA-LH27015	Coprolite		x		x				x	Unknown
MUPA-LH27140	Coprolite	x			x					Unknown
MUPA-LH23004	Coprolite		x		x					Unknown
MUPA-LH30492	Limestone				x		x	x		Unknown
MUPA-LH16605	Limestone				x			x		Drier
MUPA-LH16564	Limestone				x			x		Drier
MUPA-LH8074	Limestone				x					Wetter
MUPA-LH8172	Limestone				x		x			Wetter
MUPA-LH7202	Limestone				x					Unknown
MUPA-LH23004	Limestone				x					Unknown

99995 soil, -28.30 ‰ for $\delta^{13}\text{C}$, $+7.7$ ‰ $\delta^{15}\text{N}$; and calibrated international standards (IAEA-N1, $+0.43$ ‰ for $\delta^{15}\text{N}$; IAEA-N2, $+20.41$ ‰ for $\delta^{15}\text{N}$; IAEA-CH6, -10.50 ‰ for $\delta^{13}\text{C}$; and IAEA-CH7, -32.15 ‰ for $\delta^{13}\text{C}$; Standard deviation is ± 0.1 ‰ for $\delta^{13}\text{C}$, and ± 0.15 ‰ for $\delta^{15}\text{N}$). The samples exhibited low levels of nitrogen, so IVA 99995 soil (with 0.064 % N) was used to improve linearity of the low % N samples. The results were reported relative to Vienna Pee-Dee Belemnite (V-PDB) for carbon ($\delta^{13}\text{C}_{\text{PDB}}$) and atmospheric air for nitrogen ($\delta^{15}\text{N}_{\text{air}}$).

If sufficient coprolite remained after the untreated bulk material was analysed, the carbonates were removed to obtain the organic $\delta^{13}\text{C}$ values. The removal of the inorganic fraction ensured that the $\delta^{13}\text{C}_{\text{Org}}$ signal obtained was exclusively the carbon biological signature. The removal of inorganic carbon was carried out by covering the coprolite sample with 1M HCl in laboratory centrifuge tubes and reacting overnight (12 h) at room temperature. Samples were washed three times using distilled water and centrifuged at

3300 rpm for 5 min. Finally, the samples were dried at 60 °C for 48 h and analysed for organic $\delta^{13}\text{C}$ ($\delta^{13}\text{C}_{\text{Org}}$). Eight morphotypes (cone, cylinder, ellipsoidal, elongated, bump-headed lace, straight lace, irregular, and broken coprolites) were analysed for $\delta^{13}\text{C}_{\text{Org}}$, although bump-headed lace, elongated, and ellipsoidal morphotypes had only one specimen analysed.

Appendix B lists the isotopic and elemental data (% N, $\delta^{15}\text{N}$, % C_{tot} , and $\delta^{13}\text{C}_{\text{tot}}$ of the bulk carbon [i.e. total carbon], and % C_{Org} and $\delta^{13}\text{C}_{\text{Org}}$ after the removal of the inorganic carbon fraction) obtained from the fifty-four coprolites. The data also includes the weight before and after the removal of the inorganic carbon fraction.

3.4. Stable isotopic analyses of the limestones

Previous studies performed on the Las Hoyas laminated limestones showed that the rock had a microcrystalline structure

Table 2

Energy Dispersive X-ray (EDX) analyses on the Las Hoyas coprolites and the limestones. The number of the limestone corresponds with the coprolite specimens enclosed by the limestone. Abbreviations: BRO: Broken; CON: Cone; IRR: Irregular; LIM: Limestone; Morph: Morphotype; STR: Straight lace.

Specimen number	Morph	O	P	Ca	Al	Si	Fe	S	C	Mg	K	Na
MUPA-LH12028	BRO	51.4	9.7	30.4	0.6	0.9	0.34	0.4	6.3	–	–	–
		43.8	13.0	41.8	0.5	1.0	–	–	–	–	–	–
		42.8	11.9	43.2	0.4	0.9	–	0.6	–	–	–	–
MUPA-LH16609	CON	40.4	14.9	39.6	–	–	–	0.7	4.2	–	–	0.3
MUPA-LH16602	CON	39.8	12.7	37.8	0.6	–	–	0.6	8.5	–	–	–
MUPA-LH30492	IRR	45.1	14.1	38.7	0.4	0.7	–	0.9	–	–	–	–
		32.1	15.6	48.6	–	–	–	0.9	2.8	–	–	–
		47.3	13.8	34.4	0.5	0.8	–	0.7	2.6	–	–	–
MUPA-LH16611	STR	44.7	12.8	37.2	0.3	0.5	–	0.6	3.7	–	–	0.3
MUPA-LH30492	LIM	42.0	–	21.4	1.0	1.4	0.7	0.4	32.8	–	0.2	–
		52.4	–	36.9	0.7	1.2	–	0.3	8.4	–	–	–
		45.4	–	44.2	0.9	1.5	–	0.5	7.5	–	–	–
MUPA-LH16611	LIM	49.6	0.8	35.4	0.9	1.5	1.7	0.3	9.2	0.2	0.3	–
MUPA-LH16609	LIM	50.5	0.3	37.6	1.4	2.4	0.8	0.4	6.2	0.3	0.3	–
MUPA-LH16602	LIM	47.4	–	45.2	2.3	4.0	–	0.4	–	–	0.7	–
		53.0	–	35.8	0.8	1.2	–	–	8.8	0.33	–	–

exceeding 95 % calcite. The studies also concluded that the uniform isotopic composition of the rock micrites ($\delta^{13}\text{C} = -2.72 \pm 0.23 \text{‰}$; $\delta^{18}\text{O} = -4.81 \pm 0.17 \text{‰}$ in average) have probably preserved an isotopic composition close to that of the original calcite muds (Poyato-Ariza et al., 1998). We analysed eleven samples of limestones belonging to the wetter and drier facies, which encompassed the coprolites (Fig. 4A). Four of the samples belonged to the wetter facies and seven to the drier facies. The limestones were finely ground and homogenised using a mortar and pestle, cleaning all the tools used to avoid cross-contamination. Around 10 mg of powdered limestone was weighed for stable carbon and oxygen isotopes at the Stable Isotope Laboratory at Universidad de Salamanca (NUCLEUS), Spain. The limestones were reacted with 103 % H_3PO_4 at 25 °C, in order to produce CO_2 . The obtained gases were analysed using a Sira-II mass spectrometer (dual inlet), with an internal reference gas calibrated with different standards, including

the international standard NBS-19, and precision of $\pm 0.2 \text{‰}$ for both $\delta^{13}\text{C}$ and $\delta^{18}\text{O}$. Results were expressed in delta notation (δ), according to the equation proposed by Coplen (2011). The results were reported relative to Vienna Pee-Dee Belemnite (V-PDB) for both $\delta^{13}\text{C}$ and $\delta^{18}\text{O}$.

3.5. Criteria and features of the study

Although the TEF is usually considered to be +3.4 ‰, some previous studies suggest that a TEF of +2.5 ‰ is valid to avoid overestimating the $\delta^{15}\text{N}$ difference that occurs between the lower and higher trophic positions (Ponsard and Ardit, 2000; McCutchan et al., 2003; Vanderklift and Ponsard, 2003; Saigo et al., 2015; Serrano-Grijalva, 2015). Therefore, a wide faunal diversity and the potential trophic interaction at the Las Hoyas palaeoecosystem (Buscalioni et al., 2016) suggest that an enrichment factor for each

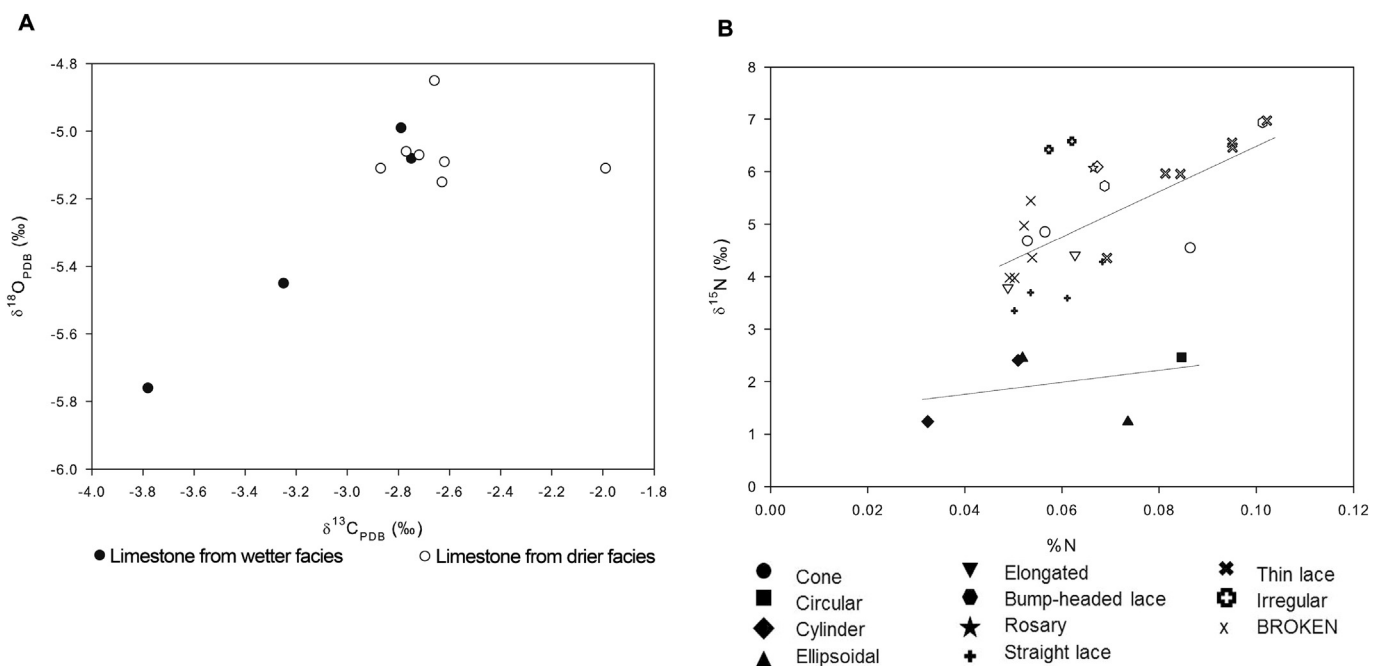


Fig. 4. Geochemical features of the host rock and the coprolites recovered from the seasonal facies. (A) Stable isotope analyses of limestones (host rock). The $\delta^{13}\text{C}$ and $\delta^{18}\text{O}$ values correspond to freshwater lakes (Leng and Marshall, 2004). (B) Covariation between $\delta^{15}\text{N}$ and % N values of the thirty-one coprolites recorded from the different seasonal facies, classified per morphotype. Coprolites from wetter facies are represented with black-filled symbols, and coprolites from drier facies are represented with white-filled symbols. The trend line represents the correlation in wetter ($r^2 = 0.10$) and drier ($r^2 = 0.41$) facies.

trophic level of 2.5 ‰ might be an appropriate TEF value. Initial identification of the baseline isotopic signatures was undertaken to establish an ecosystem food web to infer each predator's trophic position (Post, 2002; Newton, 2016). These baseline isotopic signatures vary among different types of ecosystems as reviewed by Dunne (2009), Wolf et al. (2009), Thompson et al. (2012), and Newton (2016). Unfortunately, there was no specific trophic 'baseline' discernible from the $\delta^{13}\text{C}$ or $\delta^{15}\text{N}$ values at the Las Hoyas fossil site. However, previous studies provide some reference backgrounds for the $\delta^{13}\text{C}$ values, based on the host rock and charophytes (see discussion).

For nitrogen, the lowest $\delta^{15}\text{N}$ value obtained was chosen to represent the first trophic level following the criteria of Wolf et al.

(2009). Distinct trophic levels would be assigned according to a TEF of +2.5 ‰ from the lowest $\delta^{15}\text{N}$ value. As this study is primarily interested in understanding the isotopic differences among coprolites to infer major aspects of the food web, we will not evaluate if changes in the isotopic niche distances were due to the number of sources in the food web or to the overall food web diversity (Layman et al., 2012).

3.6. Statistical analyses

To assess the comparison between stable isotope values ($\delta^{15}\text{N}$, $\delta^{13}\text{C}_{\text{tot}}$, and $\delta^{13}\text{C}_{\text{org}}$) from wet and dry conditions a t-test (normal distribution) was used. Differences between % N and % C values

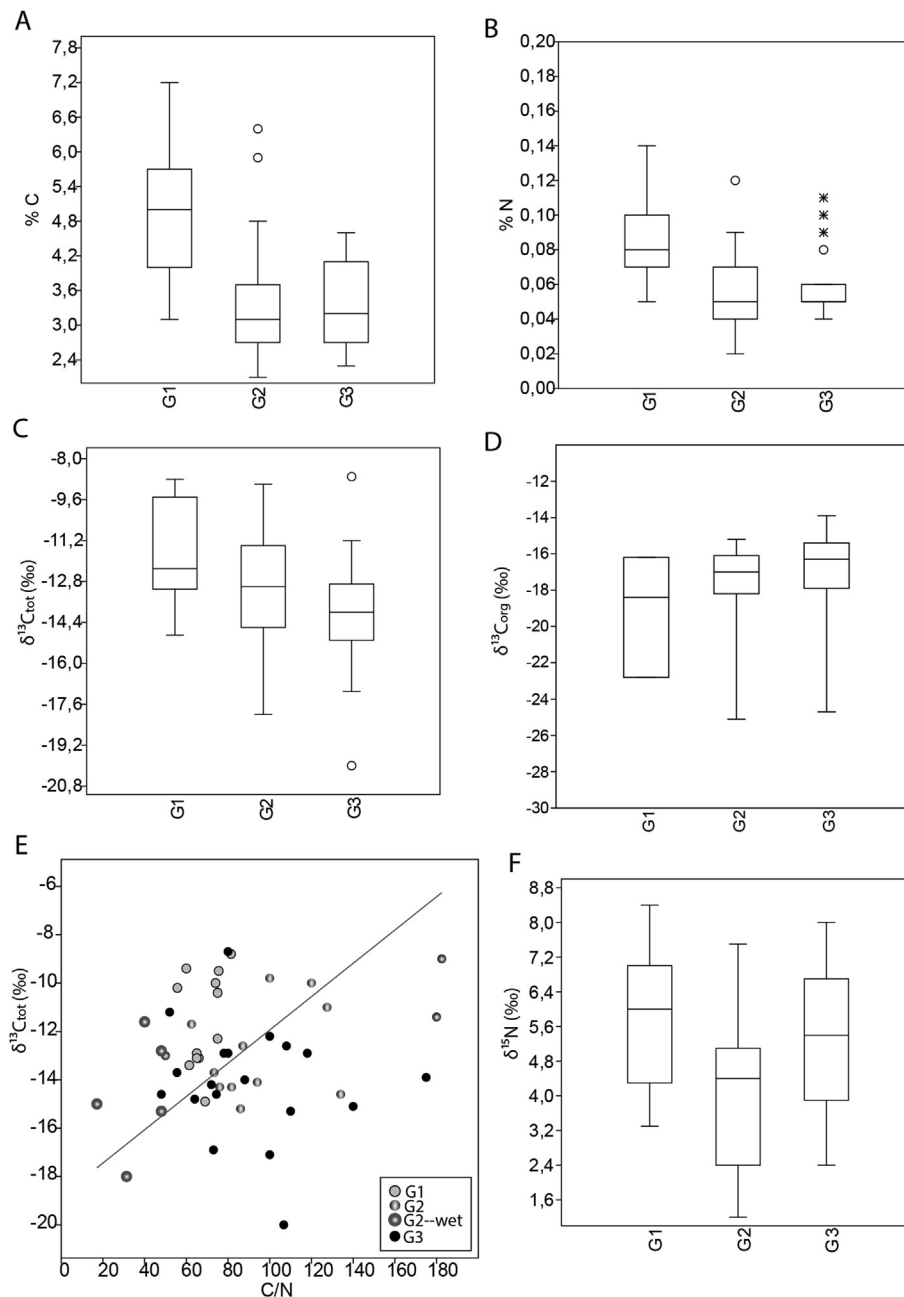


Fig. 5. Isotope variations per morphotype groups (G1 – G3). (A) Box-plot representing % C. (B) Box-plot representing % N. (C) Box-plot representing $\delta^{13}\text{C}_{\text{tot}}$. (D) Box-plot representing $\delta^{13}\text{C}_{\text{org}}$. (E) Biplot showing the covariation between $\delta^{13}\text{C}_{\text{tot}}$ and C/N. (F) Box-plot representing $\delta^{15}\text{N}$. In the box-plots, the box represents the quartiles; the line inside is the median; the whiskers represent the minimum and maximum values; the crosses and circles represent outliers.

were tested through a U-Mann Whitney test. The linear correlation coefficient is provided in the biplot of $\delta^{15}\text{N}$ and % N. Statistics have been calculated using PAST version 2.17 (Hammer et al., 2001).

4. Results

4.1. Wet and dry seasons

A bivariate plot for nitrogen (Fig. 4B), separating the specimens coming from the wet and dry facies, clearly showed two different seasonal trends. Wetter coprolites exhibited the lowest $\delta^{15}\text{N}$ values, but the % N was high. Nonetheless, the mean $\delta^{15}\text{N}$ value was significantly different to the range of values, whereas the % N was not. Differences between the mean $\delta^{15}\text{N}$ values of dry (5.1 ‰) and wet (1.9 ‰) facies samples were statistically significant: t-test, $t = -6.033$, $p = 1.6718 \cdot 10^{-6}$; while Mann-Whitney U-test, $p < 0.05$. T-tests were used to compare average % N, showing that the values of the wet and dry samples were not significant ($p = 0.251$). The coprolites recovered from the wetter facies were represented by shapes from Group 2 (i.e. ellipsoidal, circular, and cylinder). Coprolites from drier periods were more diverse in morphotype.

4.2. Carbon and nitrogen content

The isotopic variation per morphotype group is shown in Fig. 5. The mean values of % C and % N for each cluster showed that the Group 1 coprolites (composed of the lace morphotypes) were significantly different than that obtained for Groups 2 and 3 (Fig. 5A–B) (% C: $t = 3.44$, and $p = 0.0016$; and $t = 4.51$ and $p = 9.2 \cdot 10^{-5}$; % N: $t = 3.65$, $p = 0.0008$; $t = 3.32$, $p = 0.0021$, respectively). Most coprolites exhibited C/N ratios between 60 and 130 (mean 63.6, and standard deviation of 22.9). Only a few specimens (around 10 %) showed even higher values between 160 and 180, indicating a very low % N content. These latter samples corresponded to the largest coprolites assigned to Groups 3 (irregular) and 2 (cylinder) (Fig. 5B).

4.3. Carbon isotopes

The mean $\delta^{13}\text{C}_{\text{tot}}$ value of the Group 1 coprolites was significantly different from Group 2 ($t = 1.90$; $p = 0.06$) and Group 3 ($t = 3.11$, $p = 0.004$) (see Fig. 5C–D for the mean values). On a bivariate plot of $\delta^{13}\text{C}$ and C/N, the lace coprolites (Group 1) exhibited more positive $\delta^{13}\text{C}$ values (between -8 and -14 ‰), whereas the other two groups tended to be more negative (between -14 and -20 ‰). There was no correlation between $\delta^{13}\text{C}$ and C/N (Fig. 5E).

The $\delta^{13}\text{C}_{\text{org}}$ values, determined from the acid treated samples, were more negative than the $\delta^{13}\text{C}_{\text{tot}}$ values (Fig. 5D and Appendix B). These differences indicated the presence of inorganic carbon in the coprolites, due to the calcareous nature of the host rock. The analysis also confirmed that $\delta^{13}\text{C}_{\text{org}}$ was rather uniform, with the median of each group between -19 and -16 ‰ (Fig. 5D). When all morphotypes were considered, only four specimens, belonging to ellipsoidal, straight lace, broken, and irregular morphotypes exhibited the lowest $\delta^{13}\text{C}_{\text{org}}$ values (Fig. 6).

4.4. Nitrogen isotopes

The mean $\delta^{15}\text{N}$ value of Group 1 was significantly different from Group 2 ($t = 2.88$, $p = 0.0078$) but not from Group 3. The median $\delta^{15}\text{N}$ values of the groups ranged from 4.5 to 6 ‰ (Fig. 5F), with the lace coprolites having the highest values. When all morphotypes

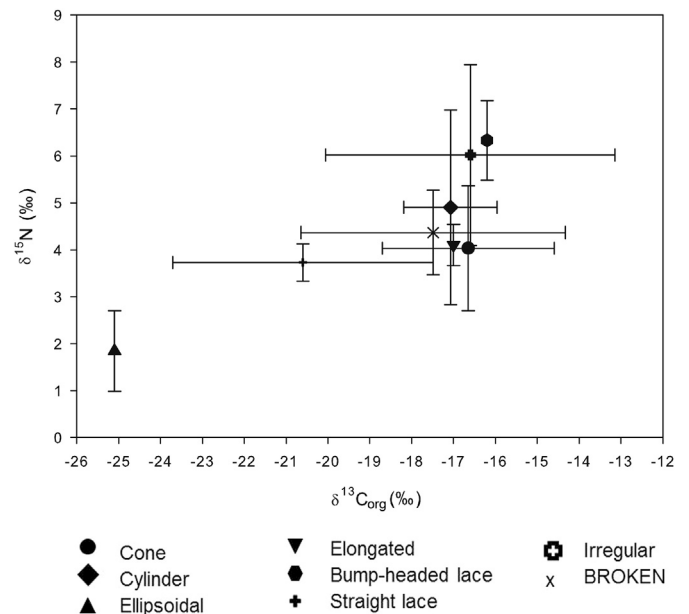


Fig. 6. Carbon and nitrogen isotopic signals. Biplot showing the covariation between $\delta^{15}\text{N}$ and $\delta^{13}\text{C}_{\text{org}}$ per morphotype analysed.

were considered, some irregular, thin lace, and cylinder coprolites showed the highest $\delta^{15}\text{N}$ values, whereas some cylinder, ellipsoidal, cone, and circular coprolites exhibited the lowest $\delta^{15}\text{N}$ values (Fig. 7).

The $\delta^{15}\text{N}$ values also increased with increasing % N content ($r^2 = 0.32$) (Fig. 7). The $\delta^{15}\text{N}$ values ranged from 1 to 8.5 ‰, indicating a variety of different trophic levels (TL) and feeding strategies for the producers of the coprolites from Las Hoyas. Thus, applying a TEF of $+2.5$ ‰, $\delta^{15}\text{N}$ values from 1.0 to 3.5 ‰ correspond to a primary trophic level, $\delta^{15}\text{N}$ values from 3.51 to 6.0 ‰ correspond to secondary trophic level, and $\delta^{15}\text{N}$ values from 6.01 to 8.5 ‰ would correspond to tertiary one.

Some morphotypes fell exclusively into a specific trophic level, probably because the number of specimens is reduced. Circular and ellipsoidal coprolites occupied the primary trophic level, elongated coprolites the secondary, and only rosary coprolites could be classified as completely belonging to the tertiary trophic level. However, specimens of other morphotypes occupied multiple trophic levels. Straight lace, bump-headed lace, cone, ellipsoidal, and elongated coprolites exhibited a range of $\delta^{15}\text{N}$ values across two trophic levels (Table 3 and Fig. 7). Cylinder and thin lace coprolites showed the highest ranges of $\delta^{15}\text{N}$ values. A high disparity of $\delta^{15}\text{N}$ values are shown by the irregular coprolites, suggesting diverse origins (Table 3).

Therefore, different specimens of the same morphotype may fall into more than one trophic level: broken coprolites had one sample within the primary trophic level, and eight specimens in the secondary level; bump-headed lace and thin lace fell into the secondary and tertiary trophic levels; cone and straight lace fell into the primary and secondary trophic levels; cylinders fell between the primary, secondary and tertiary levels; and irregular coprolites were classified within the primary and tertiary levels (see Fig. 7 and Appendix B).

Interestingly, the five largest coprolites (cylinder, irregular, and broken coprolites) neither exhibited the highest $\delta^{15}\text{N}$ values nor the highest % N. In fact, the two irregular coprolites showed some of the lowest $\delta^{15}\text{N}$ values of the sample set, whereas the 100 mm cylinder specimen represented one of the highest $\delta^{15}\text{N}$ values (Fig. 7 and Appendix B).

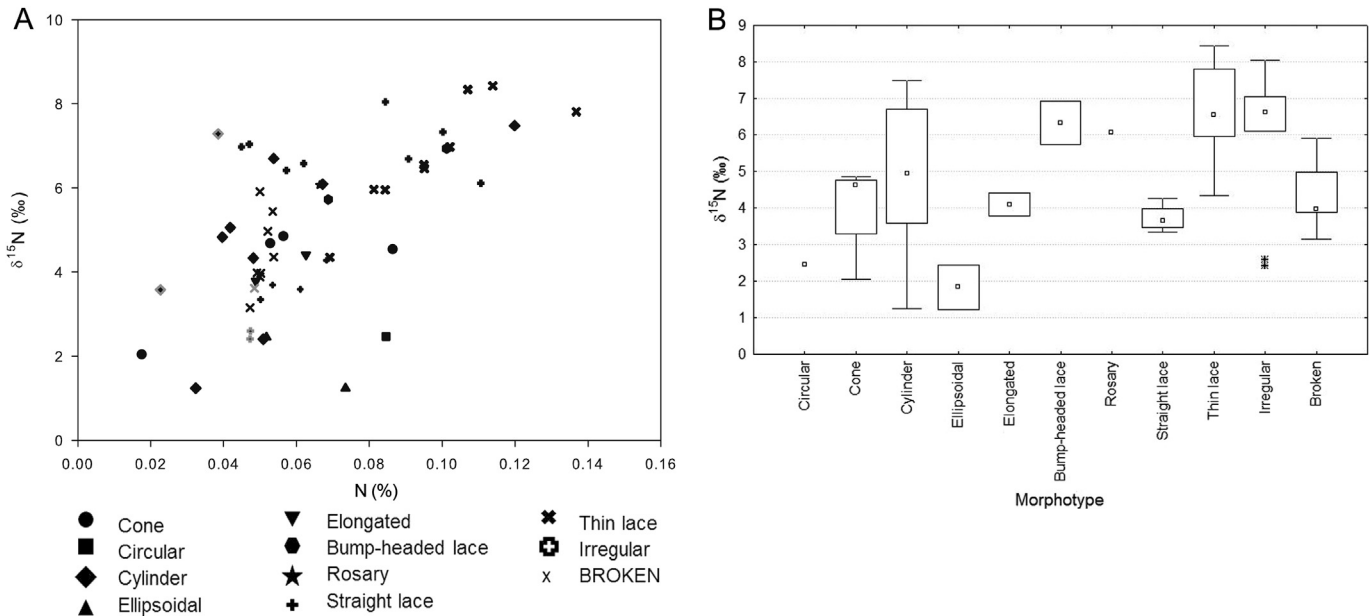


Fig. 7. Nitrogen values of the coprolites from Las Hoyas. (A) Covariation between $\delta^{15}\text{N}$ and % N. Each symbol represents a different morphotype. Larger coprolites (>40 mm in length and > 10 mm width) are outlined in grey. (B) Box-plot representing the distribution of $\delta^{15}\text{N}$ values per morphotype. Boxes represent the quartiles; the little square inside is the median; the whiskers represent the minimum and maximum values; the crosses represent the outliers. Three trophic levels are proposed for Las Hoyas ecosystem, considering a TEF of + 2.5‰: Primary consumers (1.0–3.5‰), secondary consumers (3.51–6.0‰), and tertiary consumers (6.1–8.5‰).

Table 3
Descriptive statistics for $\delta^{13}\text{C}_{\text{org}}$ and $\delta^{15}\text{N}$ values of all morphotypes analysed. Abbreviations: Morph: morphotype; N: number of coprolites; Min: minimum; Max: maximum; Range: maximum-minimum.

Morph	$\delta^{15}\text{N}$ (‰)				$\delta^{13}\text{C}_{\text{org}}$ (‰)			
	N	Mean (\pm SD)	Min	Max	N	Mean (\pm SD)	Min	Max
Circular	1	2.5	—	—	0	—	—	—
Cone	4	4.0 \pm 1.3	2.0	4.9	2	-16.6 \pm 2.0	-18.1	-15.2
Cylinder	10	4.9 \pm 2.1	1.2	7.5	7	-17.1 \pm 1.1	-18.9	-16.0
Ellipsoidal	2	1.8 \pm 0.9	1.2	2.4	1	-25.1 \pm 0	—	—
Elongated	2	4.1 \pm 0.4	3.8	4.4	1	-17.0 \pm 0	—	—
Bump-headed lace	2	6.3 \pm 0.9	5.7	6.9	1	-16.2 \pm 0	—	—
Rosary	1	6.1	—	—	0	—	—	—
Straight lace	4	3.7 \pm 0.4	3.3	4.3	2	-20.6 \pm 3.1	-22.8	-18.4
Thin lace	9	6.8 \pm 1.3	4.3	8.4	0	—	—	—
Irregular	10	6.0 \pm 1.9	2.4	8.0	3	-16.6 \pm 3.5	-20.5	-13.9
Broken	9	4.4 \pm 0.9	3.2	5.9	8	-17.5 \pm 3.1	-24.7	-13.9

5. Discussion

The facies lithology and biodiversity of Las Hoyas clearly depicts a lacustrine environment (Bascalioni and Fregenal-Martínez, 2010; Fig. 4A). Limestone $\delta^{13}\text{C}$ values of the rock embedding coprolites (ranging from -1.9 to -4 ‰) combined with negative $\delta^{18}\text{O}$ values (Fig. 4A) reinforces previous interpretations of the locality as a small-open lake influenced by karstic waters (Talbot et al., 1995; Poyato-Ariza et al., 1998). In these waters the carbonate source was derived from the dissolution of catchment limestones, and $\delta^{13}\text{C}$ values might also be influenced by the abundance of charophytes, because of their photosynthetic activity mediated the equilibrium of dissolution and precipitation of carbonates and bicarbonates (Andrews et al., 2004; Leng and Marshall, 2004). Moreover, near-bottom anoxic water is usually enriched in ^{12}C (and not ^{13}C), because it is partly derived from decomposition of terrestrial organic matter in the surface sediment (Pronin et al., 2016) which explains the lighter values of $\delta^{13}\text{C}$ measured in charophytes. The

$\delta^{18}\text{O}$ values are used to determine the distinct lithology of wet-dry facies, so that more negative $\delta^{18}\text{O}$ changes could be due to the rising water column (e.g. by temperature or rainfall) and the oxidation of organic material.

Seasonality effects are suggested in some coprolites from the wetter facies by their lower $\delta^{15}\text{N}$ signatures (Fig. 4B). Nitrogen isotope ratios are altered in wetlands during flooding, where decreasing $\delta^{15}\text{N}$ is caused by the dilution of water bodies influencing the nutrients available to the plants, the biomass available for consumers, the habitat, and growth conditions of animals and plants (Wantzen et al., 2010).

Carbon and nitrogen isotopic studies of coprolites are quite rare. In the Late Oligocene Lagerstätte of Enspel (Germany) the % C and % N coprolite values (% C = 7.45 \pm 5.85, and % N = 0.29 \pm 0.19) were lower when comparing with that of corresponding plants, insects, and tissues preserved at the same locality, but similar to the fish and tadpole bones (Schweizer et al., 2006). The Barremian coprolites from Las Hoyas showed

lower % C (mean = 3.7) and % N (mean = 0.1) values than those from the Enspel locality. The C/N ratio for the Las Hoyas coprolites association is quite homogenous, indicating a similar type of preservation, and steady state environment, as low % N would suggest an aerobic environment with more organic matter decomposition (Colombi et al., 2011).

Despite the low % C values, the $\delta^{13}\text{C}_{\text{tot}}$ values had a relative high variance (5.9) denoting that the dataset is diverse, with some morphotypes having a big variation. The $\delta^{13}\text{C}_{\text{tot}}$ values of coprolites (mean = -13.1‰) are more negative than the host rock values (-2.0 to $-3.8\text{‰} \pm 0.2$), and the mean estimated for modern charophytes of the genus *Chara* (-5.7 to -7.9‰ ; Coletta et al., 2001, and Andrews et al., 2004, respectively).

5.1. The food web context

When the covariation of $\delta^{13}\text{C}_{\text{org}}$ is expressed against $\delta^{15}\text{N}$, there is an overlap in the isotopic signatures (Fig. 6). This overlap suggests that coprolite producers would have occupied similar trophic positions, and probably competed for similar resources across one or more trophic positions or niches. The $\delta^{13}\text{C}_{\text{org}}$ values showed a large variance (8.3 ‰), ranging from -13 to -26‰ , and these values indicated a critical mid-point at -20‰ dividing the samples into two groups. This division suggests differences in the origin of the resources, which in the environmental context of Las Hoyas, $\delta^{13}\text{C}_{\text{org}} > -20\text{‰}$ would match with the dominance of animals feeding primarily on aquatic resources, and $\delta^{13}\text{C}_{\text{org}} < -20\text{‰}$ would allude to the presence of coprolites produced by animals feeding on terrestrial resources. This critical limit is congruent with $\delta^{13}\text{C}_{\text{org}}$ values obtained for different species of modern charophytes in shallow Spanish water bodies (mean = -20.7‰ for *Chara hispida*, *Nitella hyalina* and *Tolypella glomerata*; Rodrigo et al., 2016), and with the signature of the Barremian conifer *Frenelopsis* ($\delta^{13}\text{C}_{\text{org}} = -27.6\text{‰} \pm 0.9$; see Barral et al., 2017).

At least three different trophic levels for the Las Hoyas food web are proposed. The first trophic level cannot be demarcated with high certainty, as the coprolites with the lowest $\delta^{15}\text{N}$ values correspond with wetter environmental conditions (Fig. 4B). A specific baseline signature for Las Hoyas would be necessary to account for the different $\delta^{15}\text{N}$ primary producer values which, in turn, are highly variable among systems and within systems through time (Vander Zanden et al., 1997). Therefore, the proposed trophic levels are based on the assumption of a trophic enrichment factor of 2.5 ‰ for each trophic position (McCutchan et al., 2003; Vanderklift and Ponsard, 2003; Saigo et al., 2015). The vast majority of the coprolite association falls within the second trophic level. A few well-represented morphotypes (elongated, straight lace, and broken) in that level with a narrow range of $\delta^{15}\text{N}$ values suggest that the coprolite producers might have been selective feeders (specialists). However, the remainder morphotypes, including those within the third trophic level, had wider $\delta^{15}\text{N}$ ranges, and might be primary catalogued as opportunistic omnivores (animals feeding on different kinds of prey/resources according to the availability of food). The high abundance of omnivores would depict a feeding web with a high *Connectance* (i.e. the proportion of possible feeding links that are actually realized in a web), tested in ancient (Dunne et al., 2008, 2014) and in recent (Thompson et al., 2012) aquatic food webs. The Las Hoyas coprolite association may be inferred to have a flattened food web structure because of high *Connectance* (Dunne, 2009), typical in shallow water lakes and wetlands ecosystems.

5.2. Isotopic variations

The isotopic variations can be expressed relative to the coprolite size, the amount of the undigested organic matter, and the range of the nitrogen isotope values. Interestingly, the largest coprolites at Las Hoyas showed that there is no significant correlation among sizes and the isotope $\delta^{15}\text{N}$ values (Fig. 7A). The largest irregular coprolites with no visible inclusions exhibited low $\delta^{15}\text{N}$ values, which indicates that these coprolites were probably produced by medium-sized animals feeding on the basal resources of the ecosystem. Larger animals require large amounts of food to supply the necessary metabolic energy (Tucker and Rogers, 2014). On the other hand, thin and long coprolites within the lace-group (Group 1), distributed throughout the second and third trophic levels, contained abundant undigested matter in the coprolite matrices, whereas larger coprolites (e.g. the large cylinder), with similar $\delta^{15}\text{N}$ high values, did not show any bony inclusions in the matrices (Appendix B). This similar nitrogen signature in the two different groups of coprolites suggests distinctive producers. The first group might be related to fish coprolite producers with ineffective digestive processes containing abundant undigested fragments from small fishes and crustaceans prey. The second group might be related to coprolite producers having a greater digestive efficiency, such as crocodiles (Milán, 2012; Milán et al., 2018).

The variation of the coprolite carbon and nitrogen isotopic values could also be due to different climatic factors, explained by seasonality, but it could also fluctuate spatially, based on the range of preys consumed and specificity, the consumer ontogenetic stage, and individual feeding preferences (e.g. Wantzen et al., 2010; Rawlence et al., 2016; Kochi et al., 2017; Santos et al., 2018). These variations may be due to coprolites produced by opportunistic-feeding omnivores, who can increase their $\delta^{15}\text{N}$ values by supplementing their diets with occasional preys from higher trophic levels (Briand et al., 2016). Also, nitrogen ratios and trophic level may change ontogenetically within the same species, as the ability to eat larger prey changes with the increase of body/mouth size (Cohen et al., 1993). Modern adult crocodiles forage on higher trophic position prey than the non-adult individuals (Santos et al., 2018). In the same way, it is important to highlight that different animals can produce faeces with similar shape (Thulborn, 1991), and that isotopic values of consumer diets mainly reflects their feeding habits rather than their phylogeny (Briand et al., 2016).

6. Conclusions

Stable isotopes were used to evaluate the coprolite associations ($N = 54$) of an ancient ecosystem. This was an exceptional opportunity to study complex fossil remnants because of the relatively small size and diameter of the coprolites. Larger coprolites provided interesting information about the non-correspondence between size and isotopic ratios. We evaluated the results obtained using $\delta^{15}\text{N}$ and $\delta^{13}\text{C}_{\text{org}}$ isotopes to understand aspects of the food resources, trophic behaviour, and food web structure of the Las Hoyas biota, based on the isotopic signatures of their coprolites. Surprisingly, we found this ancient Barremian wetland coprolite association preserved valuable ecological information regarding specific parameters (seasonality, and differences in the nutrient levels). Obviously, some ecological parameters were blurred or difficult to determine, because the Las Hoyas site represents a complex mix of coprolites from coexisting organisms across different timescales, seasons, and spatial context. The coprolite association lacked information from the lower or basal trophic levels, which would be

represented by a plethora of taxa, such as gastropods, microcrustaceans, insects, and primary producers, which were well documented and diverse at the locality. Despite the wide scatter of the coprolite isotope signatures due to heterogeneous nature of sample material, the covariation between $\delta^{15}\text{N}$ and $\delta^{13}\text{C}_{\text{org}}$ values describe a wide spectrum across the middle and upper part of the ecosystem's food web structure. The carbon signature stressed the presence of organisms exploiting freshwater aquatic resources, and the trophic enrichment of the nitrogen isotope signal indicated at least three trophic levels for the Las Hoyas food web. Differences among the coprolite morphotypes and the variations in the $\delta^{15}\text{N}$ values, suggest that the Las Hoyas palaeoecosystem hosted specialist feeders and omnivorous and/or opportunistic feeders, the latter being the majority. Omnivory is the dominant strategy to canalize the energetic flow in shallow lacustrine ecosystems. This strategy has been maintained from ancient to modern ecosystems.

CRediT authorship contribution statement

Sandra Barrios-de Pedro: Conceptualization, Validation, Formal analysis, Investigation, Writing - original draft, Writing - review & editing, Visualization. **Karyne M. Rogers:** Methodology, Validation, Formal analysis, Investigation, Writing - review & editing, Visualization. **Paloma Alcorlo:** Formal analysis, Writing - review & editing, Visualization. **Ángela D. Buscalioni:** Conceptualization, Formal analysis, Investigation, Resources, Writing - review & editing, Visualization, Funding acquisition.

Acknowledgments

Thanks to GNS Science/Te Pu Ao (Lower Hutt, New Zealand), who provided accommodation and isotope analyses of the coprolites during a short scientific visit. Special thanks go to Andy Phillips and the team from the Stable Isotope Laboratory at GNS Science/Te Pu Ao for technical assistance. We thank to Santiago Langreo and Mercedes Llandres at the Museo de Paleontología de Castilla-La Mancha in Cuenca, for allowing us to study the coprolite collection. Many thanks go to Félix García from the Stable Isotope Laboratory at the Universidad de Salamanca (Spain) as well, for carrying out the isotope analyses of limestones. Thanks to Dr. Piotr Bajdek and Dr. Michal Zatoń, as their comments improved the original manuscript. This work was supported and financed by the Spanish Ministerio de Economía y Competitividad (MINECO) through the project CGL2013-42643P, the PhD grant BES2014-070985 associated with this project, and the travel grant EEBB-I-17-12028 "Ayudas a la movilidad predoctoral para la realización de estancias breves en centros de I+D".

References

- Ambrose, S.H., DeNiro, M.J., 1986. The isotopic ecology of East African mammals. *Oecologia* 69, 395–406. <https://doi.org/10.1007/BF00377062>.
- Andrews, J.E., Coletta, P., Pentecost, A., Riding, R., Dennis, S., Dennis, P.F., Spiro, B., 2004. Equilibrium and disequilibrium stable isotope effects in modern charophyte calcites: implications for palaeoenvironmental studies. *Palaeogeography, Palaeoclimatology, Palaeoecology* 204, 101–114. [https://doi.org/10.1016/S0031-0182\(03\)00725-9](https://doi.org/10.1016/S0031-0182(03)00725-9).
- Bailleul, A., Ségalen, L., Buscalioni, A.D., Cambra-Moo, O., Cubo, J., 2011. Palaeohistology and preservation of tetrapods from Las Hoyas (Lower Cretaceous, Spain). *Comptes Rendus Palevol* 10, 367–380. <https://doi.org/10.1016/j.crpv.2011.05.002>.
- Bajdek, P., Owocki, K., Niedzwiedzki, G., 2014. Putative dicynodont coprolites from the Upper Triassic of Poland. *Palaeogeography, Palaeoclimatology, Palaeoecology* 411, 1–17. <https://doi.org/10.1016/j.palaeo.2014.06.013>.
- Bajdek, P., Qvarnström, M., Owocki, K., Sulej, T., Sennikov, A.G., Golubev, V.K., Niedzwiedzki, G., 2016. Microbiota and food residues including possible evidence of pre-mammalian hair in Upper Permian coprolites from Russia. *Lethaia* 49, 455–477.
- Bajdek, P., Owocki, K., Sennikov, A.G., Golubev, V.K., Niedzwiedzki, G., 2017. Residues from the Upper Permian carnivore coprolites from Vyazniki in Russia—Key questions in reconstruction of feeding habits. *Palaeogeography, Palaeoclimatology, Palaeoecology* 482, 70–82.
- Barral, A., Gomez, B., Fourel, F., Daviero-Gomez, V., Lécuyer, C., 2017. CO₂ and temperature decoupling at the million-year scale during the Cretaceous Greenhouse. *Scientific Reports* 7. <https://doi.org/10.1038/s41598-017-08234-0> article number 8310.
- Barrios-de Pedro, S., 2019. Integrative study of the coprolites from Las Hoyas (upper Barremian; La Huérguina Formation, Cuenca, Spain). Unpublished PhD Thesis. Universidad Autónoma de Madrid, Spain, p. 400.
- Barrios-de Pedro, S., Buscalioni, A.D., 2018. Scrutinizing barremian coprolite inclusions to record digestive strategies. *Annales Societatis Geologorum Poloniae* 88 (2), 203–221. <https://doi.org/10.14241/asgp.2018.014>.
- Barrios-de Pedro, S., Poyato-Ariza, F.J., Moratalla, J.J., Buscalioni, A.D., 2018. Exceptional coprolite association from the Early Cretaceous continental Lagerstätte of Las Hoyas, Cuenca, Spain. *PLoS One* 13 (5), E0196982. <https://doi.org/10.1371/journal.pone.0196982>.
- Briand, M.J., Bonnet, X., Guillou, G., Letourneur, Y., 2016. Complex food webs in highly diversified coral reefs: Insights from $\delta^{13}\text{C}$ and $\delta^{15}\text{N}$ stable isotopes. *Food Webs* 8, 12–22. <https://doi.org/10.1016/j.fooweb.2016.07.002>.
- Briggs, D.E.G., Wilby, R., Pérez-Moreno, B.P., Sanz, J.L., Fregenal-Martínez, M.A., 1997. The mineralization of dinosaur soft tissue in the Lower Cretaceous of Las Hoyas, Spain. *Journal of the Geological Society, London* 154, 587–588.
- Briggs, D.E.G., Gupta, N.S., Cambra-Moo, O., 2016. Molecular preservation. In: Poyato-Ariza, F.J., Buscalioni, A.D. (Eds.), *Las Hoyas: A Cretaceous wetland*. Dr. Friedrich Pfeil Verlag, München, Germany, pp. 216–219.
- Buscalioni, A.D., Fregenal-Martínez, M., 2010. A holistic approach to the palaeoecology of Las Hoyas Konservat-Lagerstätte. In: Buscalioni, A.D., Fregenal-Martínez, M.A. (Eds.), *Journal of Iberian Geology, Spec. vol. 36* (2), 297–326. *Mesozoic Terrestrial Ecosystems and Biotas*. https://doi.org/10.5209/rev_JIGE.2010.v36.n2.13.
- Buscalioni, A.D., Poyato-Ariza, F.J., 2016. Las Hoyas: A unique Cretaceous ecosystem. In: Khosla, A., Lucas, S.G. (Eds.), *Cretaceous Period: Biotic Diversity and Biogeography*. New Mexico Museum of Natural History and Science, pp. 51–63. Bulletin 71.
- Buscalioni, A.D., Poyato-Ariza, F.J., Marugán-Lobón, J., Fregenal-Martínez, M.A., Sanisidro, O., Navalón, G., Miguel, C. de, 2016. The wetland of Las Hoyas. In: Poyato-Ariza, F.J., Buscalioni, A.D. (Eds.), *Las Hoyas: A Cretaceous wetland*. Dr. Friedrich Pfeil Verlag, München, Germany, pp. 238–253.
- Caut, S., Angulo, E., Courchamp, F., 2009. Variation in discrimination factors ($\delta^{15}\text{N}$ and $\delta^{13}\text{C}$): the effect of diet isotopic values and applications for diet reconstruction. *Journal of Applied Ecology* 46, 443–453. <https://doi.org/10.1111/j.1365-2664.2009.01620.x>.
- Chin, K., Gill, B.D., 1996. Dinosaurs, dung beetles, and conifers: Participants in a Cretaceous Food Web. *PALAIOS* 11, 280–285. <https://doi.org/10.2307/3515235>.
- Chin, K., Kirkland, J.I., 1998. Probable herbivore coprolites from the Upper Jurassic Mygatt-Moore Quarry, Western Colorado. *Modern Geology* 23, 249–275.
- Chin, K., Tokaryk, T.T., Erickson, G.M., Calk, L.C., 1998. A king-sized theropod coprolite. *Nature* 393, 680–682. <https://doi.org/10.1038/31461>.
- Cohen, J.E., Pimm, S.L., Yodanis, P., Saldaña, J., 1993. Body sizes of animal predators and animal prey in food webs. *Journal of Animal Ecology* 62, 67–78. <https://doi.org/10.2307/5483>.
- Coletta, P., Pentecost, A., Spiro, B., 2001. Stable isotopes in charophyte incrustations: relationships with climate and water chemistry. *Palaeogeography, Palaeoclimatology, Palaeoecology* 173 (1–2), 9–19. [https://doi.org/10.1016/S0031-0182\(01\)00305-4](https://doi.org/10.1016/S0031-0182(01)00305-4).
- Colombi, C.E., Montañez, I.P., Parrish, J.T., 2011. Registro de la relación isotópica de carbono en la paleoflora de la Formación Ischigualasto (Triásico Superior), Noroeste Argentino: Implicaciones Paleoatmosféricas. *Revista Brasileira de Paleontología* 14 (1), 1–12. <https://doi.org/10.4072/rbp.2011.1.04>.
- Combes, C., Cazalbou, S., Rey, C., 2016. Apatite Biominerals. *Minerals* 6 (2). <https://doi.org/10.3390/min6020034> article number 34.
- Coplen, T.B., 2011. Guidelines and recommended terms for expression of stable-isotope-ratio and gas-ratio measurement results. *Rapid Communications in Mass Spectrometry* 25, 2538–2560.
- Cosmidis, J., Benzerara, K., Guyot, F., Skouri-Panet, F., Duprat, E., Féraud, C., Guigner, J.-M., Bonnaubeau, F., Coelho, C., 2015. Calcium-phosphate biominer- alization induced by alkaline phosphatase activity in *Escherichia coli*: Localization, kinetics, and potential signatures in the fossil record. *Frontiers of Earth Science* 3. <https://doi.org/10.3389/feart.2015.00084> article number 84.
- DeNiro, M.J., Epstein, S., 1978. Influence of diet on the distribution of carbon isotopes in animals. *Geochimica et Cosmochimica Acta* 42, 495–506. [https://doi.org/10.1016/0016-7037\(78\)90199-0](https://doi.org/10.1016/0016-7037(78)90199-0).
- DeNiro, M.J., Epstein, S., 1981. Influence of diet on the distribution of nitrogen isotopes in animals. *Geochimica et Cosmochimica Acta* 45, 341–351. [https://doi.org/10.1016/0016-7037\(81\)90244-1](https://doi.org/10.1016/0016-7037(81)90244-1).
- Diéguez, C., Martín-Closas, C., Meléndez, N., Rodríguez-Lázaro, J., Trínçao, P., 1995. *Biostratigraphy: Las Hoyas, A Lacustrine Konservat-Lagerstätte, Field Trip guide book*. Universidad Autónoma de Madrid, pp. 77–79.

- Dunne, J.A., Williams, R.J., Martínez, N.D., Wood, R.A., Erwin, D.H., 2008. Compilation and network analyses of Cambrian food webs. *PLoS Biology* 6 (4). <https://doi.org/10.1371/journal.pbio.0060102> e102.
- Dunne, J.A., 2009. Food Webs. In: Myers, R.A. (Ed.), *Encyclopedia of Complexity and Systems Science*. Springer, New York, USA, pp. 3361–3682. <https://doi.org/10.1007/978-0-387-30440-3>.
- Dunne, J.A., Labandeira, C.C., Williams, R.J., 2014. Highly resolved early Eocene food webs show development of modern trophic structure after the end-Cretaceous extinction. *Proceedings of the Royal Society of London B: Biological Sciences* 281. <https://doi.org/10.1098/rspb.2013.3280>.
- Eggers, T., Jones, T.H., 2000. You are what you eat. . . or are you? *Trends in Ecology & Evolution* 15, 265–266. [https://doi.org/10.1016/S0169-5347\(00\)01877-2](https://doi.org/10.1016/S0169-5347(00)01877-2).
- Fishman, M.R., Giglio, K., Fay, D., Filiatrault, M.J., 2018. Physiological and genetic characterization of calcium phosphate precipitation by *Pseudomonas* species. *Scientific Reports* 8, 10156. <https://doi.org/10.1038/s41598-018-28525-4>.
- Fregenal-Martínez, M.A., 1998. Análisis de la cubeta sedimentaria de Las Hoyas y su entorno paleogeográfico (Cretácico Inferior, Serranía de Cuenca). *Sedimentología y aspectos tafonómicos del yacimiento de Las Hoyas*. Unpublished PhD Thesis. Universidad Complutense de Madrid, Spain, p. 354.
- Fregenal-Martínez, M.A., Meléndez, N., 2000. The lacustrine fossiliferous deposits of the Las Hoyas sub-basin (lower Cretaceous, Serranía de Cuenca, Iberian Ranges, Spain). In: Gierlowski-Kordesch, E.H., Kelts, K. (Eds.), *Lake basins through space and time*. AAPG Studies in Geology, vol. 46, pp. 303–314.
- Fregenal-Martínez, M.A., Muñoz-García, M.B., Buscalioni, A.D., Elez, J., de la Horra, R., 2014. The karstic habitat of Spelaogriphaceans from the Las Hoyas fossil site (Upper Barremian, Serranía de Cuenca, Spain). In: Rocha, R., Pais, J., Kullberg, J., Finney, S. (Eds.), *STRATI 2013*. Springer Geology, pp. 1175–1179.
- Fregenal-Martínez, M.A., Meléndez, N., 2016. Environmental reconstruction: a historical review. In: Poyato-Ariza, F.J., Buscalioni, A.D. (Eds.), *Las Hoyas: A Cretaceous wetland*. Dr. Friedrich Pfeil Verlag, München, Germany, pp. 14–28.
- Fregenal-Martínez, M.A., Meléndez, N., Muñoz-García, M.B., Elez, J., de la Horra, R., 2017. The stratigraphic record of the Late Jurassic–Early Cretaceous rifting in the Alto Tajo-Serranía de Cuenca region (Iberian Ranges, Spain): genetic and structural evidences for a revision and a new lithostratigraphic proposal. *Revista de la Sociedad Geológica de España* 30 (1), 113–142.
- Fricke, H.C., Rogers, R.R., Backlund, R., Dwyer, C.N., Echt, S., 2008. Preservation of primary stable isotope signals in dinosaurs remains, and environmental gradients of the Late Cretaceous of Montana and Alberta. *Palaeogeography, Palaeoclimatology, Palaeoecology* 266, 13–27. <https://doi.org/10.1016/j.palaeo.2008.03.030>.
- Ghosh, P., Bhattacharya, S.K., Sahni, A., Kar, R.K., Mohabey, D.M., Ambwani, K., 2003. Dinosaur coprolites from the Late Cretaceous (Maastrichtian) Lameta Formation of India: isotopic and other markers suggesting a C₃ plant diet. *Cretaceous Research* 24, 743–750. <https://doi.org/10.1016/j.cretres.2003.08.002>.
- Hammer, O., Harper, D.A.T., Ryan, P.D., 2001. *PAST: Paleontological Statistics software package for education and analysis*. *Palaeontologia Electronica* 4 (1), 9.
- Hollocher, K.T., Alcober, O.A., Colombi, C.E., Hollocher, T.C., 2005. Carnivore coprolites from the Upper Triassic Ischigualasto Formation, Argentina: Chemistry, Mineralogy, and Evidence for rapid initial mineralization. *PALAIOS* 20, 51–63. <https://doi.org/10.2110/palo.2003.p03-98>.
- Hollocher, K.T., Hollocher, T.C., Rigby Jr., K., 2010. A phosphatic coprolite lacking diagenetic permineralization from the Upper Cretaceous Hell Creek Formation, Northeastern Montana: importance of dietary calcium phosphate in preservation. *PALAIOS* 25, 132–140. <https://doi.org/10.2110/palo.2008.p08-132r>.
- Hollocher, K., Hollocher, T.C., 2012. Early processes in the fossilization of terrestrial feces to coprolites, and microstructure preservation. In: Hunt, A.P., Milán, J., Lucas, S.G., Spielmann, J.A. (Eds.), *Vertebrate coprolites*. New Mexico Museum of Natural History and Science, pp. 79–91. *Bulletin* 57.
- Iniesto, M., López-Archilla, A.I., Fregenal-Martínez, M.A., Buscalioni, A.D., Guerrero, M.C., 2013. Involvement of microbial mats in delayed decay: An experimental essay on fish preservation. *PALAIOS* 28, 56–66. <https://doi.org/10.2110/palo.2011.p11-099r>.
- Iniesto, M., Buscalioni, A.D., Guerrero, M.C., Benzerara, K., Moreira, D., López-Archilla, A.I., 2016. Involvement of microbial mats in early fossilization by decay delay and formation of impressions and replicas of vertebrates and invertebrates. *Scientific Reports* 6, 1–12. <https://doi.org/10.1038/srep25716>.
- Iniesto, M., Blanco-Moreno, C., Villalba, A., Buscalioni, A.D., Guerrero, M.C., López-Archilla, M.A., 2018. Plant tissue decay in long-term experiments with microbial mats. *Geosciences* 8 (11), 387. <https://doi.org/10.3390/geosciences8110387>.
- Kling, G.W., Fry, B., O'Brien, W.J., 1992. Stable isotopes and planktonic trophic structure in Arctic Lakes. *Ecology* 73 (2), 561–566. <https://doi.org/10.2307/1940762>.
- Kochi, S., Pérez, S.A., Tessone, A., Ugan, A., Tafuri, M.A., Nye, J., Tivoli, A.M., Zangrando, A.F., 2017. $\delta^{13}\text{C}$ and $\delta^{15}\text{N}$ variations in terrestrial and marine food webs of Beagle Channel in the Holocene. Implications for human paleodietary reconstructions. *Journal of Archaeological Science Reports*. <https://doi.org/10.1016/j.jasrep.2017.11.036>.
- Kolasinski, J., Rogers, K., Frouin, P., 2008. Effects of acidification on carbon and nitrogen stable isotopes of benthic macrofauna from a tropical coral reef. *Rapid Communications in Mass Spectrometry* 22, 2955–2960. <https://doi.org/10.1002/rcm.3694>.
- Krause, J.M., Piña, C.I., 2012. Reptilian coprolites in the Eocene of Central Patagonia, Argentina. *Journal of Paleontology* 86 (3), 527–538. <https://doi.org/10.1002/jpa.20086>.
- Lamboley, M., Purnachandra Rao, V., Ahmed, E., Azzouzi, N., 1994. Nanostructure and significance of fish coprolites in phosphorites. *Marine Geology* 120, 373–383. [https://doi.org/10.1016/0025-3227\(94\)90068-X](https://doi.org/10.1016/0025-3227(94)90068-X).
- Layman, C.A., Araujo, M.S., Boucek, R., Hammerschlag-Peyer, C.M., Harrison, E., Jud, Z.R., Matich, P., Rosenblatt, A.E., Vaudo, J.J., Yeager, L.A., Post, D.M., Bearhop, S., 2012. Applying stable isotopes to examine food web structure: an overview of analytical tools. *Biological Reviews of the Cambridge Philosophical Society* 87, 545–562. <https://doi.org/10.1111/j.1469-185X.2011.00208.x>.
- Leng, M.J., Marshall, J.D., 2004. Palaeoclimate interpretation of stable isotope data from lake sediment archives. *Quaternary Science Reviews* 23, 811–831. <https://doi.org/10.1016/j.quascirev.2003.06.012>.
- McCutchan Jr., J.H., Lewis Jr., W.M., Kendall, K., McGrath, C.C., 2003. Variation in trophic shift for stable isotope ratios of carbon, nitrogen, and sulfur. *Oikos* 102, 378–390. <https://www.jstor.org/stable/3548040>.
- Milán, J., 2012. Crocodylian scatology—A look into morphology, internal architecture, inter- and intraspecific variation and prey remains in extant crocodylian feces. In: Hunt, A.P., Milán, J., Lucas, S.G., Spielmann, J.A. (Eds.), *Vertebrate coprolites*. New Mexico Museum of Natural History and Science, pp. 65–72. *Bulletin* 57.
- Milán, J., Rasmussen, E.S., Dybkjaer, K., 2018. A crocodylian coprolite from the lower Oligocene Viborg Formation of Sofienlund Lergrav, Denmark. *Bulletin of the Geological Society of Denmark* 66, 181–187.
- Minagawa, M., Wada, E., 1984. Stepwise enrichment of ^{15}N along food chains: Further evidence and the relation between $\delta^{15}\text{N}$ and animal age. *Geochimica et Cosmochimica Acta* 48, 1135–1140. [https://doi.org/10.1016/0016-7037\(84\)90204-7](https://doi.org/10.1016/0016-7037(84)90204-7).
- Newton, J., 2016. *Stable isotopes as tools in ecological research*. Wiley J. and Sons Ltd., Chichester. <https://doi.org/10.1002/9780470015902.a0021231.pub2>.
- Northwood, C., 2005. Early Triassic coprolites from Australia and their palaeobiological significance. *Palaeontology* 48 (1), 49–68. <https://doi.org/10.1111/j.1475-4983.2004.00432.x>.
- Peñalver, E., Gaudant, J., 2010. Limnic food web and salinity of the Upper Miocene Biocorb palaeolake (Eastern Spain). *Palaeogeography, Palaeoclimatology, Palaeoecology* 297, 683–696. <https://doi.org/10.1016/j.palaeo.2010.09.017>.
- Ponsard, S., Ardití, R., 2000. What can stable isotopes ($\delta^{15}\text{N}$ and $\delta^{13}\text{C}$) tell about the food web of soil macro-invertebrates? *Ecology* 81 (3), 852–864.
- Post, D.M., 2002. Using stable isotopes to estimate trophic position: models, methods and assumptions. *Ecology* 83 (3), 703–718. <https://doi.org/10.2307/3071875>.
- Poyato-Ariza, F.J., Talbot, M.R., Fregenal-Martínez, M.A., Meléndez, N., Wenz, S., 1998. First isotopic and multidisciplinary evidence for nonmarine coelacanths and pycnodontiform fishes: palaeoenvironmental implications. *Palaeogeography, Palaeoclimatology, Palaeoecology* 144 (1–2), 65–84.
- Pronin, E., Pelechaty, M., Apolinarska, K., Pukacz, A., Frankowski, M., 2016. Sharp differences in the $\delta^{13}\text{C}$ values of organic matter and carbonate encrustations but not in ambient water DIC between two morphologically distinct charophytes. *Hydrobiologia* 773 (1), 177–191. <https://doi.org/10.1007/s10750-016-2698-6>.
- Rawlence, N.J., Wood, J.R., Bocherens, H., Rogers, K.M., 2016. Dietary interpretations for extinct megafauna using coprolites, intestinal contents and stable isotopes: Complementary or contradictory? *Quaternary Science Reviews* 142, 173–178. <https://doi.org/10.1016/j.quascirev.2016.05.017>.
- Rodrigo, M.A., García, A., Chivas, A., 2016. Carbon stable isotope composition of charophyte organic matter in small and shallow Spanish water body as a baseline for future trophic studies. *Journal of Limnology* 75 (2), 226–235. <http://ro.uow.edu.au/smhpapers/3993>.
- Rodríguez-de la Rosa, R.A., Cevallos-Ferriz, S.R.S., Silva-Pineda, A., 1998. Paleobiological Implications of Campanian coprolites. *Palaeogeography, Palaeoclimatology, Palaeoecology* 142, 231–254. [https://doi.org/10.1016/s0031-0182\(98\)00052-2](https://doi.org/10.1016/s0031-0182(98)00052-2).
- Saigo, M., Zilli, F.L., Marchese, M.R., Demonte, D., 2015. Trophic level, food chain length and omnivory in the Paraná River: a food web model approach in a floodplain river system. *Ecological Research* 30, 843–852. <https://doi.org/10.1007/s11284-015-1283-1>.
- Santos, X., Navarro, S., Campos, J.C., Sanpera, C., Brito, J.C., 2018. Stable isotopes uncover trophic ecology of the West African crocodile (*Crocodylus suchus*). *Journal of Arid Environments* 148, 6–13. <https://doi.org/10.1016/j.jaridenv.2017.09.008>.
- Schlacher, T.A., Connolly, R.M., 2014. Effects of acid treatment on carbon and nitrogen stable isotope ratios in ecological samples: a review and synthesis. *Methods in Ecology and Evolution* 5, 541–550.
- Schoeninger, M.J., DeNiro, M.J., 1984. Nitrogen and carbon isotopic composition of bone collagen from marine and terrestrial animals. *Geochimica et Cosmochimica Acta* 48 (4), 625–639. [https://doi.org/10.1016/0016-7037\(84\)90091-7](https://doi.org/10.1016/0016-7037(84)90091-7).
- Schweizer, M.K., Wooller, M.J., Toporski, J., Fogel, M.L., Steele, A., 2006. Examination of an Oligocene lacustrine ecosystem using C and N stable isotopes. *Palaeogeography, Palaeoclimatology, Palaeoecology* 230, 335–351. <https://doi.org/10.1016/j.palaeo.2005.06.038>.
- Schweizer, M.K., Steele, A., Toporski, J.K., Fogel, M.L., 2007. Stable isotopic evidence for fossil food webs in Eocene Lake Messel. *Paleobiology* 33 (4), 590–609. <https://www.jstor.org/stable/4500174>.
- Serrano-Grijalva, L., 2015. Efectos del cambio global en la estructura trófica de los humedales a través del uso de isótopos estables. PhD Dissertation. Museo Nacional de Ciencias Naturales (CSIC), Madrid, p. 196. <http://hdl.handle.net/10261/127832>.
- Sugama, T., Pyatina, T., 2018. Alkali-activated cement composites for high temperature geothermal wells. *Scientific Research Publishing, Inc., USA*, p. 262.

Talbot, M.R., Meléndez, N., Fregenal-Martínez, M.A., 1995. The waters of the Las Hoyas lake: Sources and limnological characteristics. In: Meléndez, N. (Ed.), *Las Hoyas, A lacustrine Konservat-Lagerstätte*, Cuenca, Spain. Universidad Complutense, Madrid, pp. 11–16.

Thompson, R.M., Dunne, J.A., Woodward, G.U.Y., 2012. Freshwater food webs: towards a more fundamental understanding of the biodiversity and community dynamics. *Freshwater Biology* 57 (7), 1329–1341. <https://doi.org/10.1111/j.1365-2427.2012.02808.x>.

Thulborn, R.A., 1991. Morphology, preservation and palaeobiological significance of dinosaur coprolites. *Palaeogeography, Palaeoclimatology, Palaeoecology* 83, 341–366. [https://doi.org/10.1016/0031-0182\(91\)90060-5](https://doi.org/10.1016/0031-0182(91)90060-5).

Tucker, M.A., Rogers, T.L., 2014. Examining predator-prey body size, trophic level and body mass across marine and terrestrial mammals. *Proceedings of the Royal Society Biological Science* 281, 1–10. <https://doi.org/10.1098/rspb.2014.2103>.

Vanderklift, M.A., Ponsard, S., 2003. Sources of variation in consumer-diet d15N enrichment; a meta-analysis. *Oecologia* 136, 169–182. <https://doi.org/10.1007/s00442-003-1270-z>.

Vander Zanden, M.J., Cabana, G., Rasmussen, J.B., 1997. Comparing the trophic position of littoral fish estimated using stable nitrogen isotopes ($\delta^{15}N$) and dietary data. *Canadian Journal of Fisheries and Aquatic Sciences* 54 (5), 1142–1158. <https://doi.org/10.1139/cjfas-54-5-1142>.

Vander Zanden, M.J., Shuter, B.J., Lester, N., Rasmussen, J.B., 1999. Patterns of food chain length in lakes: a stable isotope study. *The American Naturalist* 154, 406–416. <https://doi.org/10.1086/303250>.

Vander Zanden, M.J., Rasmussen, J.B., 2001. Variation in $15N$ and $13C$ trophic fractionation: implications for aquatic food web studies. *Limnology & Oceanography* 46, 2061–2066. <https://doi.org/10.4319/lo.2001.46.8.2061>.

Vander Zanden, M.J., Fetzner, W.W., 2007. Global patterns of aquatic food chain length. *Oikos* 116, 1378–1388. <https://doi.org/10.1111/j.0030-1299.2007.16036.x>.

Vicente, A., Martín-Closas, C., 2013. Lower Cretaceous charophytes from the Seranía de Cuenca, Iberian chain: Taxonomy, biostratigraphy and palaeoecology. *Cretaceous Research* 40, 227–243. <https://doi.org/10.1016/j.cretres.2012.07.006>.

Wantzen, K.M., Fellerhoff, C., Voss, M., 2010. Stable isotope ecology of the food webs of the Pantanal. In: Junk, W.J., Da Silva, C.J., Nunes da Cunha, C., Wantzen, K.M.

(Eds.), *The Pantanal: Ecology, biodiversity and sustainable management of a large neotropical seasonal wetland*. Pensoft Publisher, Sofia, Moscow, pp. 597–616.

Wolf, N., Carleton, S.A., del Rio, C.M., 2009. Ten years of experimental animal isotopic ecology. *Functional Ecology* 23 (1), 17–26.




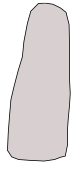


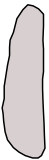
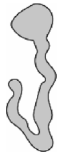

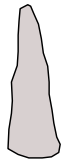
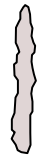

Zazzo, A., Lécuyer, C., Mariotti, A., 2004. Experimentally-controlled carbon and oxygen isotope exchange between bioapatites and water under inorganic and microbially-mediated conditions. *Geochimica et Cosmochimica Acta* 68 (1), 1–12. [https://doi.org/10.1016/S0016-7037\(03\)00278-3](https://doi.org/10.1016/S0016-7037(03)00278-3).

Ziegler, A.M., Raymond, A.L., Gierlowski, T.C., Horrel, M.A., Rowley, D.B., Lottes, A.L., 1987. Coal, climate and terrestrial productivity: the present and the Early Cretaceous compared. In: Scott, A.C. (Ed.), *Coal and Coal-bearing Strata: Recent advances*, vol. 32. Geological Society of London Special Publications, pp. 25–49.

Appendix A. Supplementary data

Supplementary data to this article can be found online at <https://doi.org/10.1016/j.cretres.2019.104343>.

Appendix A. The upper Barremian coprolite association from Las Hoyas (Cuenca, Spain). Every morphotype includes a description and a drawing. The lower line corresponds to some features of the morphotype: OS: Overall shape; Ou: Outline; ES: End shapes; KI: Kind of inclusions. Information and drawings obtained from Barrios-de Pedro and Buscalioni (2018), and Barrios-de Pedro et al. (2018).

Spiral	Circular	Irregular	Elongated	Rosary	Ellipsoidal
With spiral marks. Strips with regular widths on the surface.	Rather flat, lentil-like, but not as flat as a disc.	Undefined, features not share between specimens; varied mosaic of shapes.	Straight longitudinal axis without noticeable volume (usually flat).	Series of wide segments with bumps separated by constrictions.	Wider at the middle, major axis twice or three times longer than minor axis. Without special elongation.
					
OS: Elongated Ou: Straight ES: Differs among specimens KI: No inclusions or unidentified inclusions	OS: Rounded Ou: Curved and irregular ES: Not defined KI: Bony inclusions (fish vertebrae and scales)	OS: Undefined Ou: Varied ES: Not applicable KI: Depends on the specimen: no inclusions, plants or bony inclusions	OS: Rectangular Ou: Straight ES: Isopolar, flat ends KI: Fish scales and other bony inclusions	OS: Segmented into bumps Ou: Sinuous ES: Isopolar, rounded KI: Both thin and thick bony inclusions	OS: Roughly ovoid Ou: Straight ES: Isopolar, rounded KI: Depends on the specimen: no inclusions, plants or bony inclusions
Cylinder	Bump-headed lace	Fir-tree	Cone	Straight lace	Thin lace
Longitudinal axis roughly constant in width. With volume.	One end with a big bulge, at least twice as wide as the rest.	Sequence of 'bumps' decreasing progressively from wide to a very narrow end.	Increasing in diameter towards one end. Without constrictions.	Long, straight, unfolded; with similar diameter throughout the length.	Folded onto themselves, with a roughly identical diameter. Shape is ribbon-like.
					
OS: Elongated Ou: Straight to slightly curved ES: Isopolar, rounded KI: Mainly bony inclusions	OS: Elongated cord with a bulge Ou: Sinuous ES: Anisopolar, large bulge at one end KI: Bony elements (probably scales) and rings (probably vertebrae)	OS: Triangular Ou: Sinuous ES: Anisopolar, smaller end rounded and bigger end almost straight KI: Scales and other bony inclusions	OS: Cone to tear-drop Ou: Straight ES: Anisopolar, smaller end a bit sharp or rounded, and bigger end almost straight KI: Bony inclusions and possible ostracods	OS: Elongated cord Ou: Sinuous ES: Anisopolar, one end always rounded and the other flat to sharp KI: Scales and thin bony inclusions	OS: Ribbon-like Ou: Sinuous ES: Anisopolar, one end sharp and the other flat or rounded KI: Thread-like structures, rings (probably vertebrae) and bony inclusions

Appendix B. List of all the specimens analysed, including the morphotype, length, width (the smallest diameter of the coprolite), relative diameter (length/width), the type of facies from every coprolite was collected, and the isotopic data (% N, $\delta^{15}\text{N}$, % C, and $\delta^{13}\text{C}$ of the total carbon [i.e., organic and inorganic fraction; % C_{tot} and $\delta^{13}\text{C}_{\text{tot}}$], and the same values after the removal of the inorganic carbon fraction [i.e., % C_{org} and $\delta^{13}\text{C}_{\text{org}}$]). Abbreviations: RD: Relative diameter; WBT: Weight before acid treatment; WAT: Weight after acid treatment.

Specimen number	Morphotype	Length (mm)	Width (mm)	RD	Facies	%N	$\delta^{15}\text{N}$	% C_{tot}	$\delta^{13}\text{C}_{\text{tot}}$	% C_{org}	$\delta^{13}\text{C}_{\text{org}}$	WBT (mg)	WAT (mg)
MUPA-LH8172 (12)	Circular	10	4.0	2.5	Wetter	0.08	2.5	2.7	-18.0	-	-	-	-
MUPA-LH16517	Cone	5	2.0	2.5	Drier	0.09	4.5	5.9	-13.0	-	-	-	-
MUPA-LH16602	Cone	10	4.0	2.5	Drier	0.06	4.9	3.1	-14.3	2.7	-18.1	34.9	9.9
MUPA-LH16609	Cone	15	6.0	2.5	Drier	0.05	4.7	3.7	-14.1	-	-	-	-
MUPA-LH-GQ17-010	Cone	20	6.0	3.3	Unknown	0.02	2.0	2.3	-9.8	1.6	-15.2	32.3	10.1
MUPA-LH8074	Cylinder	9	3.0	3.0	Wetter	0.03	1.2	2.9	-11.6	2.2	-18.9	10.8	2.1
MUPA-LH8175	Cylinder	13	2.5	5.2	Wetter	0.05	2.4	3.8	-12.8	2.4	-18.2	21.1	8.6
MUPA-LH8048 (2)	Cylinder	16	2.0	8.0	Drier	0.07	6.1	4.8	-12.6	-	-	-	-
MUPA-LH-GQ15-001	Cylinder	9	2.0	4.5	Unknown	0.12	7.5	6.4	-11.7	-	-	-	-
MUPA-LH21486	Cylinder	46	8.0	5.8	Unknown	0.05	4.3	2.7	-15.2	2.5	-17.0	31.2	10.1
MUPA-LH9475	Cylinder	50	14.0	3.6	Unknown	0.02	3.6	3.5	-11.4	-	-	-	-
MUPA-LH9651	Cylinder	100	16.0	6.3	Unknown	0.04	7.3	3.6	-9.0	2.5	-16.2	32.8	9.9
MUPA-LH-GQ17-011	Cylinder	20	8.0	2.5	Unknown	0.04	5.1	2.5	-11.0	2.2	-16.1	31.6	9.8
MUPA-LH-GQ17-013	Cylinder	26	8.0	3.3	Unknown	0.05	6.7	2.8	-14.6	2.6	-17.1	30.1	9.9
MUPA-LH-GQ17-014	Cylinder	30	9.0	3.3	Unknown	0.04	4.8	3.0	-10.0	2.2	-16.0	34.6	9.9
MUPA-LH8172 (11)	Ellipsoidal	24	11.0	2.2	Wetter	0.05	2.4	2.1	-15.3	3.0	-25.1	34.2	2.3
MUPA-LH8174	Ellipsoidal	6	3.0	2.0	Wetter	0.07	1.2	2.9	-15.0	-	-	-	-
MUPA-LH16516	Elongated	10	5.5	1.8	Drier	0.05	3.8	3.4	-14.3	2.4	-17.0	31.5	10.0
MUPA-LH8048 (1)	Elongated	6	3.5	1.7	Drier	0.06	4.4	3.7	-13.7	-	-	-	-
MUPA-LH8048 (4)	Bump-headed lace	15	1.0	15.0	Drier	0.10	6.9	4.5	-14.9	-	-	-	-
MUPA-LH8036	Bump-headed lace	46	1.5	30.7	Drier	0.07	5.7	5.0	-8.8	4.7	-16.2	10.3	4.3
MUPA-LH16531	Rosary	20	2.0	10.0	Drier	0.08	6.1	-	-	-	-	-	-
MUPA-LH8048 (6)	Straight lace	11	3.0	3.7	Drier	0.09	4.3	3.4	-13.4	-	-	-	-
MUPA-LH8092	Straight lace	30	3.0	10.0	Drier	0.05	3.7	3.6	-10.0	2.8	-18.4	29.1	10.0
MUPA-LH16603	Straight lace	25	2.0	12.5	Drier	0.05	3.3	3.1	-13.1	3.7	-22.8	7.7	0.5
MUPA-LH16611	Straight lace	13	2.0	6.5	Drier	0.06	3.6	5.3	-9.4	-	-	-	-
MUPA-LH16590	Thin lace	25	1.5	16.7	Drier	0.10	6.5	5.2	-12.9	-	-	-	-
MUPA-LH16564	Thin lace	20	2.0	10.0	Drier	0.07	4.3	-	-	-	-	-	-
MUPA-LH16557	Thin lace	28	1.0	28.0	Drier	0.08	6.0	4.3	-10.4	-	-	-	-
MUPA-LH8133	Thin lace	12	1.25	9.6	Drier	0.10	6.5	5.7	-13.1	-	-	-	-
MUPA-LH16585	Thin lace	32	1.5	21.3	Drier	0.08	6.0	4.0	-12.3	-	-	-	-
MUPA-LH16548	Thin lace	28	2.0	14.0	Drier	0.10	7.0	-	-	-	-	-	-
MUPA-LH-LI15-028	Thin lace	29	1.0	29.0	Unknown	0.14	7.8	6.8	-10.2	-	-	-	-
MUPA-LH-GQ15-007	Thin lace	14	1.50	9.3	Unknown	0.11	8.4	6.5	-	-	-	-	-
MUPA-LH-GQ15-003	Thin lace	14	1.0	14.0	Unknown	0.11	8.3	7.2	-9.5	-	-	-	-
MUPA-LH8014 (2)	Irregular	11	4.0	2.8	Drier	0.06	6.6	4.3	-15.3	-	-	-	-
MUPA-LH8192	Irregular	11	6.0	1.8	Drier	0.06	6.4	4.3	-20.0	-	-	-	-
MUPA-LH-GQ15-004	Irregular	7	2.5	2.8	Unknown	0.11	6.1	4.1	-13.7	-	-	-	-
MUPA-LH-GQ15-008	Irregular	8	2.5	3.2	Unknown	0.10	7.3	3.3	-16.9	-	-	-	-
MUPA-LH-LI15-011	Irregular	17	5.0	3.4	Unknown	0.09	6.7	3.2	-14.6	-	-	-	-
MUPA-LH7202	Irregular	100	32.0	3.1	Unknown	0.05	2.4	2.7	-14.6	2.2	-15.4	34.0	10.1
MUPA-LH23004	Irregular	67	39.0	1.7	Unknown	0.05	2.6	2.5	-11.2	1.9	-13.9	34.1	9.8
MUPA-LH27015	Irregular	33	15.0	2.2	Unknown	0.04	7.0	2.9	-13.9	3.2	-20.5	10.7	0.9
MUPA-LH27140	Irregular	20	6.0	3.3	Unknown	0.08	8.0	4.5	-17.1	-	-	-	-
MUPA-LH30492	Irregular	25	11.0	2.3	Unknown	0.05	7.0	3.0	-15.1	-	-	-	-
MUPA-LH8038	Broken	10	5.0	2.0	Drier	0.05	5.0	4.0	-12.2	2.6	-17.6	36.5	9.9
MUPA-LH16601	Broken	20	2.0	10.0	Drier	0.05	5.4	3.3	-12.6	5.0	-24.7	36.0	2.5
MUPA-LH16607	Broken	-	-	-	Drier	0.05	4.0	4.6	-8.7	-	-	-	-
MUPA-LH16594	Broken	-	8.0	-	Drier	0.05	4.0	2.9	-12.9	2.4	-16.3	35.1	10.3
MUPA-LH16605	Broken	13	10.0	1.3	Drier	0.05	4.4	3.3	-14.0	2.5	-17.9	33.3	10.1
MUPA-LH9195	Broken	-	-	-	Unknown	0.05	3.9	2.3	-12.9	1.9	-13.9	34.0	10.0
MUPA-LH12028	Broken	55	19.0	2.9	Unknown	0.05	3.6	2.8	-14.2	2.1	-16.2	32.0	9.9
MUPA-LH20240	Broken	35	26.0	1.3	Unknown	0.05	3.2	2.5	-14.8	2.0	-17.0	32.0	9.9
MUPA-LH-GQ17-012	Broken	26	7.0	3.7	Unknown	0.05	5.9	2.7	-12.9	2.3	-16.3	34.9	10.1

Appendix C. Diagenetic alterations and taphonomy of coprolites and the host rock.

The rock

Previous studies on the Las Hoyas laminated limestones showed that the substrate has a microcrystalline structure, exceeding 95 % calcite (Poyato-Ariza et al., 1998). Crystals vary from submicron-size micrite to a coarse microspar mosaic with individual calcite crystals up to 25 mm. The non-carbonate components correspond to phosphatic products derived from vertebrate fossils and coprolites, and to organic material of both aquatic and terrestrial origin, depending on the fossil. A study performed by Poyato-Ariza et al. (1998) determined that the main effect of carbonate diagenesis in the locality is present as sparry infills that showed lower $\delta^{13}\text{C}$ values ($\sim -7\text{‰}$) than the host limestones. However, they concluded that the uniform composition of the rock micrites (mean values; $\delta^{13}\text{C} = -2.72 \pm 0.23\text{‰}$, $\delta^{18}\text{O} = -4.81 \pm 0.17\text{‰}$) suggests that their isotopic composition is close to that of the original limestone muds. Some of the coprolite host rock from this study was analysed in order to evaluate the carbon and oxygen isotopic signals of these limestones (see Fig. 4A and Section 3.4.) belonging to the wetter and drier facies. The $\delta^{13}\text{C}$ and $\delta^{18}\text{O}$ values indicated that the samples correspond to freshwater lakes (Leng and Marshall, 2004), reflecting humidity and oxidation of large amounts of organic material in the ecosystem.

The coprolites

It has not been fully explained yet whether the diagenesis of the coprolite apatite is similar to that of other bioapatites, such as bones, enamel, or dentine (Fricke et al., 2008). The diagenetic alteration of these bodily remains depends on: (1) decomposition of the organic matter, (2) the change in the chemical composition by trapping ions (fluoride or heavy elements) that may affect the amount of isotopic exchange between fluids and the biogenic apatite, and (3) the dissolution, recrystallization, and/or addition of secondary minerals (Zazzo et al., 2004; Combes et al., 2016).

Faeces are the natural decomposition and degradation product of ingested organic matter. In faecal mass mineralization occurs rapidly, and its early lithification process deals with a phosphatic coprolite matrix with a uniform crystalline nanostructure (Hollocher et al., 2010; Krause and Piña, 2012). The lithification process is assisted by the presence of a diverse group of intestinal or environmental bacteria promoting the formation of biominerals and incorporation of carbonates into the apatite lattice (Lambooy et al., 1994; Hollocher et al., 2010; Krause and Piña, 2012; Bajdek et al., 2016). The mediation of microorganisms (e.g., bacteria, fungi) in the carbonate and phosphate precipitation is a viable possibility. Other studies (Chin and Kirkland, 1998; Cosmidis et al., 2015; Fishman et al., 2018) propose that the incorporation of apatite carbonate ions greatly depends on the concentration of carbonate in the precipitating medium.

The taphonomic properties of the Las Hoyas coprolites show that they were mostly produced in an aqueous milieu, and probably soaked before burial, in carbonate alkaline water. Regarding the composition of their apatite varieties (see Section 3.2), the inclusion of fluoride (carbonated-fluorapatite: francolite) in some samples (MUPA-LH9195), might be discussed either as the dissolution of bone content in the primary coprolite matrix or as a chemical modification of dahllite during diagenesis (Hollocher et al., 2005). The acquisition of fluoride can occur by ion exchange with groundwater and it does not require recrystallization or deposition of a new mineral phase (Hollocher et al., 2010). Another component, the hydroxylapatite sulfonated is an intermediate phase of degraded apatite (Sugama and Pyatina, 2018). Thus, in some specimens, a subtle alteration on the chemical composition is probable. Concerning secondary precipitation and recrystallization, veins of coarse sparite grains were not detected in Las Hoyas coprolites; instead, the coprolite matrix is uniform, comprising a microcrystalline matrix, with no hint of phosphatic recrystallization (Barrios-de Pedro, 2019).

Accordingly, we attempt to establish that diagenesis has not entirely obscured the original stable isotope values obtained after the chemical pre-treatment. Nonetheless, we are conscious that isotopic analyses are more common on other inorganic structures, such as enamel (Zazzo et al., 2004), and to date, there is extremely limited amount of data reported from other bioapatite materials, such as coprolites.